NASA-CR-135091
PWA-5386

PRELIMINARY COMPRESSOR DESIGN STUDY FOR AN ADVANCED MULTISTAGE AXIAL FLOW COMPRESSOR F'NAL REPORT

by
H. V. Marman and R. D. Marchant

September 1976

PRATT & WHITNEY AIRCRAFT GROUP
Commercial Products Division

prepared for

NATIONAL AERONAUTICS AND SPACE ADMINISTRATION

NASA-Lewis Research Center
Contract NAS3-19445

1 Report No	2 Government Accession No	3 Recipient's Catalog No
NASA CR-135091		

4 Title and Subtitle	5 Report Date
Preliminary Compressor Design Study for an Advanced Multistage Axial Flow Compressor – Final Report	September 1976
	6 Performing Organization Code

7 Author(s)	8 Performing Organization Report No
H. V. Marman and R. D. Marchant	PWA-5386
	10 Work Unit No

9 Performing Organization Name and Address	11 Contract or Grant No
Pratt & Whitney Aircraft Group Commercial Product Division United Technologies Corporation East Hartford, CT. 06108	NAS3-19445
	13 Type of Report and Period Covered
12 Sponsoring Agency Name and Address	Contractor Report
National Aeronautics and Space Administration Washington, D. C. 20546	14 Sponsoring Agency Code

15 Supplementary Notes

Project Manager: R. S. Ruggeri, Fluid System Components Division, Fan and Compressor Branch, NASA-Lewis Research Center, Cleveland, Ohio 44135

16 Abstract

A parametric study was conducted to define an optimum, axial-flow, high-pressure ratio compressor for a turbofan engine for commercial subsonic transport service starting in the late 1980's. The study was based on projected 1985 technologies. The study effort was applied to compressors with an 18:1 pressure ratio and having 6 to 12 stages. A matrix of 49 compressors was developed by statistical techniques. The compressors were evaluated by means of computer programs in terms of various airline economic figures-of-merit such as return-on-investment and direct-operating-cost. The optimum configuration was determined to be a high speed, 8-stage compressor with an average blading aspect ratio of 1.15.

17 Key Words (Suggested by Author(s))	18 Distribution Statement
High-Pressure Compressor Commercial Transport Aircraft 1985 Technology Airline Economics	Unclassified – Unlimited

19 Security Classif (of this report)	20 Security Classif (of this page)	21 No of Pages	22 Price*
Unclassified	Unclassified		

* For sale by the National Technical Information Service, Springfield, Virginia 22151

FOREWARD

This report describes work performed by the Pratt & Whitney Aircraft Group, Commercial Products Division, United Technologies Corporation, for the National Aeronautics and Space Administration, NASA-Lewis Research Center under Contract NAS3-19445. During this effort Mr. R.S. Ruggeri was the NASA Project Manager and Mr. H. V. Marman was the P&WA Program Manager. The report was prepared by H. V. Marman and R.D. Marchant with contributions from J.W. Bisset, F.E. Dauser, B. A. Robideau, and other P&WA personnel.

TABLE OF CONTENTS

TABLE OF CONTENTS (Cont'd)

LIST OF ILLUSTRATIONS

LIST OF ILLUSTRATIONS (Cont'd)

PRELIMINARY COMPRESSOR DESIGN STUDY FOR AN ADVANCED MULTISTAGE AXIAL FLOW COMPRESSOR FINAL REPORT

H. V. Marman and R. D. Marchant

SUMMARY

A parametric study was conducted to define an optimum, axial-flow, high-pressure compressor for an advanced turbofan engine for use in a commercial subsonic transport which will go into service late in the 1980's. The study was based on an aggressive projection of 1985 technology. The aircraft, mission, and base engine (designated STF477) were obtained from an earlier NASA program (NAS3-19132). This earlier program also identified the engine cycle and engine configuration best meeting the requirements of the aircraft and mission. The optimization study effort was applied to a high-pressure compressor with an 18:1 pressure ratio and having 6 to 12 stages.

The compressor configurations were evaluated in terms of various figures-of-merit (FOM) such as airline return-on-investment (ROI), direct-operating-cost (DOC), and fuel-burned (FB). For the study, a matrix of 49 high-pressure compressor configurations was developed by statistical techniques. These configurations were processed by means of a computer program from which high-pressure compressor efficiency and geometry were determined. A regression analysis was performed on the efficiency data to determine the configuration with the optimum efficiency and the relative sensitivity of efficiency to the parametric design variables.

Thirty-four compressors from the matrix were weighed and costed and substituted in the base engine. All base engine components were adjusted for each of the new compressors to insure that all engines had the same thrust; the primary FOM's were then calculated. A regression analysis of ROI data was performed to determine the compressor configuration with the maximum ROI.

The high-pressure compressors with the best ROI were compared with those having optimum efficiency. Three optimum configurations were selected and processed, weighed, and costed. From this study two new compressors meeting structural requirements of blading resonance and flutter margin were selected. These two configurations were then reviewed. In this review, maintenance cost and technology risk were considered. Based on this analysis and calculated ROI, a high speed, 8-stage compressor with an average aspect blading ratio of 1.15 was determined to be optimum.

The aggressive technology projections made for 1985 led to a significantly improved compressor design having fewer stages and fewer number of parts while yielding a higher airline return-on-investment and lower fuel-burned. Maintenance costs and airfoil-deterioration-life significantly influenced system economics. The optimum configuration, which has a comparatively low aspect ratio, is attractive both for performance and for system economics.

INTRODUCTION

A parametric study was conducted to define an optimum, axial-flow, high-pressure ratio compressor for an advanced turbofan aircraft engine. The engine is for application in a commercial, subsonic transport that would enter service in the late 1980's and would provide maximum economic benefits to the airlines. The study utilized technology aggressively projected to be available in circa 1985.

The aircraft, mission, and base engine (designated STF477) employed in the program were obtained from an earlier NASA-sponsored study (ref. 1). In addition this earlier study identified the engine cycles and configurations best meeting the requirements imposed by the assumed aircraft and mission. This earlier study showed that an overall engine cycle pressure ratio of 40:1 or greater, leading to a core compressor pressure ratio of at least 18:1, is necessary to achieve the required performance, fuel consumption, weight, and return-on-investment.

The high-pressure (HP) compressor has a strong influence on overall engine design, weight, and performance; on the design of other components; on fuel consumption; and on aircraft return-on-investment. Compressor efficiency strongly affects thrust-specific-fuel-consumption and to a lesser degree affects engine size, weight, and cost. As examples: The HP compressor losses (efficiency) directly contribute to turbine work requirements and influence the quality (e.g., temperature) of the air bleed for turbine cooling. High-pressure compressor exit conditions (airflow profile and Mach number) influence the diffuser and combustor configuration, length, and pressure loss. In addition the length, weight, and configuration of the HP compressor directly affect the number and arrangement of the rotor shaft bearings and the critical speed of the entire high-pressure spool.

Along with high values of efficiency, it is essential that significant reductions in the number of stages be achieved in order to reduce compressor cost and weight. The advanced HP compressor must also demonstrate stable operation over a wide range of conditions. In addition, the HP compressor must be reliable and durable, and provide satisfactory performance over a long period of service.

The optimum compressor for the subject study program is defined in terms of the overall engine (viz. the optimum compressor is the compressor in the optimum overall engine) which in turn is defined in terms of the requirements of the overall aircraft and mission. Because of the interaction of the compressor with the other engine components, principally the combustor and turbines, designing the optimum high-pressure compressor is a difficult task involving compromises in many areas. The objective of the study program was to select the aggressive high-pressure compressor design that is optimum (as defined) for the intended service. The level of technology projected for all areas of the engine (STF477) is similar to that projected for the compressor (i.e., 1985 technology).

The parametric study involved a large number of high-pressure designs. To compare these designs, aircraft and engine economic "figures-of-merit" were established; and statistical techniques were developed for selecting optimum configurations in terms of the engine figures-of-merit. By computer techniques, thousands of high-pressure compressor designs were incorporated in the advanced base-engine and evaluated in terms of the typical mission in the designated aircraft. Based on the results of this evaluation and other detailed aerodynamic and structural reviews, the optimum (airline) return-on-investment HP compressor configuration that met all performance and structural requirements was selected.

PRELIMINARY CONSIDERATIONS

The effect of HP compressor efficiency on fuel-burned (FB) and airline return-on-investment (ROI) is presented in Figures 1 and 2 for a constant cruise thrust and a constant exhaust nozzle jet velocity ratio (Vj duct/Vj primary).† As shown, the influence of HP compressor efficiency on FB and airline ROI is substantial. Most of the improvement in FB and ROI with increased efficiency results from reductions in thrust-specific-fuel-consumption (TSFC). The additional improvements are obtained from changes in engine cycle which permit a reduction in size, weight, and cost of the engine. For example: A one percent increase in HP compressor efficiency at constant combustor exit temperature and a constant exhaust nozzle jet velocity ratio can provide a 0.5% decrease in TSFC, a 0.9% increase in cruise thrust, and a 1.5% increase in cycle bypass ratio. The increase in thrust permits the entire engine to be scaled down in size for the same aircraft/mission requirements. This scaling down, combined with the increased bypass ratio, results in a reduction in engine weight, core size, and price with only a slight increase in fan diameter. These effects are shown in Figure 3 as functions of HP compressor efficiency.

Fuel costs and efficiency, although of major importance, are not the only considerations that will affect the economic success of future transports. A breakdown of direct-operating-costs (DOC) of a typical, advanced, commercial four-engine airplane is shown below for the assumed fuel price of $0.45/gal.

Fuel	31%*
Crew	19%
Aircraft Price	19%
Engine Maintenance	14%*
Aircraft Maintenance	10%
Engine Price	7%*

*Engine related costs

Maintenance and other direct-operating-costs are influenced by reliability and the cost of replacement parts. Fewer, more durable, and less costly parts lead to a reduction in maintenance costs and also development costs. Greater durability of the high-pressure compressor can also reduce direct-operating-costs by minimizing performance deterioration and thus maintain minimum TSFC for a longer portion of the serviceable life of the engine. The economic importance of maintenance and reliability has been manifested by recent NASA studies (ref. 2 and 3).

The program was initiated by establishing the aircraft and base engine to be utilized in the study. The engine component technology for the 1985 time period was then projected.

†Abbreviations and symbols are defined in Appendix A.

REPRESENTATIVE AIRCRAFT

Commercial marketing projections indicate a potential need for an aircraft entering service in the 1980's that meets the constraints of minimum energy consumption and low cost of ownership, low noise, and low emissions. The NASA sponsored "Study of Turbofan Engines Designed for Low Energy Consumption", Contract NAS3-19132, identified a representative aircraft that conforms to these constraints and its expected missions (ref. 1). This aircraft and its mission formed the basis for the compressor screening studies. The aircraft and mission are described below.

AIRCRAFT

- Engine: 4 turbofans
- Passengers: 200
- TOGW: 131,000 kg [288,000 lbm]

MISSION

- Design range: 10,200 km [5,500 n. mi.]
- Typical stage length: 3,700 km [2,000 n. mi.]
- Cruise Mach number: 0.80
- Required field length: 3,200 m [10,500 ft]

Advanced technology features in this aircraft include supercritical aerodynamics, extensive application of composites, and high aspect ratio wings, all of which contribute to reduced fuel usage. The design Mach number of 0.80 represents a trade between minimum time-in-flight considerations and minimum fuel consumption.

REPRESENTATIVE ENGINE

The baseline engine selected for the high-pressure compressor optimization studies was identified during the NASA-sponsored study (ref. 1) as the engine best meeting the requirements imposed by the representative aircraft and mission. This engine, a turbofan configuration designated STF477, resulted from studies made within the context of the projected 1985 state-of-the-art technologies in all engine component areas including controls and nacelle-engine integration.

The STF477 engine has a 45:1 overall pressure ratio cycle, a HP compressor pressure ratio of 18:1, and a bypass ratio of 8:1. The fan pressure ratio is 1.7:1; the low-pressure compressor ratio is about 1.47:1; and the maximum combustor exit temperature is 1470°C [2600°F]. The high-pressure compressor is driven by a two-stage turbine. The fan/low-pressure compressor consists of a fan stage and three compressor stages, and is driven by a five-stage turbine. A cross-section drawing of the STF477 is presented by Figure 4.

ESTABLISHMENT OF 1985 STATE-OF-THE-ART

The selection of the optimum compressor is contingent upon achieving levels of technology which are aggressive but believed to be attainable by 1985. The state-of-the-art levels utilized were projected from present levels and were based on current and planned programs and P&WA experience. The projected advancements in the state-of-the-art are necessary to achieve the required engine system performance, weight, and economic benefits.

The technological areas in which the projections were made are: high-pressure compressor, fan, low-pressure compressor, combustor, turbines, structures, materials, controls, fabrication processing, acoustics, and engine-nacelle integration.

High-Pressure Compressor Technology Projections

Blade Losses

The losses in a compressor blade row consist of viscous and shock losses. The viscous losses are a combination of blade profile (blade boundary layer) losses and endwall (wall boundary layer) losses. For inlet flows below the critical Mach number, the losses consist of only viscous losses; above the critical Mach number, shock losses are also included. Reducing these losses increases compressor efficiency and blade loading capability.

In transonic and supersonic blading, profile and shock losses are coupled through complex shock-boundary-layer interactions on the surfaces where shocks impinge. To reduce these blade losses, technology developed for fan systems will be employed. The fan system utilizes multiple-circular-arc (MCA) airfoils which provide a means for controlling blade shapes to give a lower loss than more conventional airfoil shapes. Low loss levels with MCA blading have been consistently achieved at higher Mach numbers in tests of fans. It is anticipated that the reduction in total loss forecast for the transonic blading in the higher Mach number regions of the HP compressors will result from use of the MCA airfoils; conventional series airfoils (i.e., CA, 400, 65) were assumed for subsonic regions.

Blade and Endwall Loading Limits

The limit of stable operation of a compressor blade row is a function of the aerodynamics of both the blading and the annulus endwalls. Loading limits exist for blade and endwall boundary layers, which if exceeded results in a flow instability (stall) within a given blade row. The complexity of the viscous three-dimensional flow in a compressor blade passage has to date prevented development of an accurate method of predicting the limiting pressure grandients. For current HP compressors, the blade and endwall loading limits have been found to correlate principally with blade aspect ratio and endwall boundary layer displacement thickness. Correlations of loading have been established which show the influence of aspect ratio on multistage compressor stability. These correlations, albeit incomplete, can be used where detailed boundary layer data are not available.

Blade Loading Limits: Diffusion factor (D-factor)† is widely used to define cascade loading and to correlate cascade data. These correlated data have been used to determine (approximately) the surge-limited, maximum loading attainable with a given aspect ratio in any stage of a multistage compressor. Recent test data indicate that a six percent increase in average blade-loading over current levels can be attained. A six percent improved loading was assumed for the advanced technology high-pressure compressor.

Endwall Loading Limits: In the absence of sufficient endwall boundary layer data, endwall loading limits were predicted based on empirical correlations of loading as a function of aspect ratio. The endwall loading† limits forecast for advanced compressors are seven percent greater than permitted by present technology.

Stability

Reductions in compressor surge margin requirements are anticipated for advanced commercial transport engines. These reductions are expected through improvements in the compressor surge-line characteristics and distortion sensitivity and through improvements in the engine control system. Control system improvements which affect surge margin requirements are expected in areas related to manufacturing tolerances, schedule tracking accuracy, and deterioration.

The minimum required surge margin for an advanced technology compressor at the design point was estimated to be 15 percent. The 15 percent requirement was dictated by the combined influence of surge margin requirements at specific critical operating conditions and the estimated characteristics of the surge line and operating line.

Improved Tip Clearances

Improved performance will also result from tighter running clearances (combined with higher tip speeds) at the tip of the rotor and at the root of the cantilevered stators. Reductions in current running clearances will lead to reduced seal leakage and, thus, improvements in efficiency. These reductions in clearances will be possible because of increased understanding of the transient thermal behavior of the rotor and case structure, improved abradable and abrasive rub strips to minimize the effect of rubs during aircraft maneuvers, better rotor dynamic design techniques, the use of damped bearings to increase rotor stability, and the application of passive and dynamic tip clearance controls where necessary. Average running clearances of 0.25 mm [0.010 in.] are expected.

Other Component Technology Projections

Fan Technology

Projected advances in fan technology will permit reduction of airfoil and endwall losses without degrading aeroelastic integrity. More efficient controlled-shock blading will be used in place of the present multiple-circular arc blading to reduce shock losses. Improvements or elimination of interblade shrouds used to control blade flutter will reduce losses in these regions of the gaspath.

†Defined in Appendix B

Low-Pressure Compressor Technology

Improved stability margin and efficiency are the primary advancements projected for the low-pressure compressor. Improvements with respect to loading capability, noise, weight, and manufacturing cost are also expected. Tighter gaspath sealing at blade tips and other leakage parts will reduce losses.

Combustor Technology

An advanced, high-temperature, high-pressure, low-emissions combustor with a low-loss inlet diffuser will be matched to the compressor and turbine.

High-Pressure Turbine Technology

The high-pressure turbine will have a higher efficiency with an increased rotor speed. New, lighter-weight blade designs will reduce the centrifugal load on the blades caused by the higher rotor speeds. Losses will be reduced by tighter gaspath sealing and reduced disk windage (gas-disk friction) effects. Nondeteriorating, static, abradable seals of metallic and ceramic materials and improved rotating component abrasive materials suitable for use with the abradable seals are forecast. As in the compressor, active clearance control may be used in the high-pressure turbine to control blade tip clearances.

Low-Pressure Turbine Technology

Projected technology advances will provide a low-pressure turbine with a high load factor to minimize the number of stages and reduce stage losses. Laminar flow airfoils will reduce the blading losses. Active clearance control will be utilized to minimize running clearances.

Structural-Mechanical Technology

Rotor speeds well beyond current levels will be required to take advantage of projected improvements in aerodynamics and materials. These increased speeds will, in turn, require improvements in several structural-mechanical areas, two examples of which are lightweight turbine blades and advanced bearings and seals.

The lightweight turbine blades will be required to reduce centrifugal stresses on the blade attachments. The use of advanced titanium alloys in place of nickel-based alloys in the aft stages is a possibility.

Higher rotor speeds coupled with increased pressure levels will require significant advances in main engine bearings and bearing compartment seals. Bearing DN levels (bearing bore diameter times speed – mm X rpm) approaching 3,000,000 and main seal face speeds of 180 m/sec [600 ft/sec] are examples.

Materials Technology

Improved materials will be required for all major components of the advanced engine. These materials will provide increased strength-to-density ratios and higher temperature capabilities. Improvements are expected in areas of coatings, directional solidified eutectic materials, titanium-aluminide intermetallics, cobalt and dispersion strengthened nickel alloys, composites, and ceramics.

Control Technology

To satisfy the requirements of the advanced aircraft and engine, an electronic control system was chosen. The technologies projected for this system are increased accuracy, improved sensitivity and reaction time, and better communication between aircraft and engine. The capability to manage the large number of loops required by the advanced engine was also projected. Although the requirements of the advanced application are highly complex, the utilization of electronics is expected to maintain control system weight at current levels. In addition, electronic controls should be less costly while being more flexible and reliable. Maintenance costs are also expected to be less because of the ability of the control to perform self-check functions.

Fabrication and Processing Technology

Advancements in fabrication and processing technologies are required to meet the projected manufacturing cost goals. Development programs underway should yield the technologies to accomplish these goals. Computer-aided design and manufacturing development programs were projected to reduce design, tooling, machining, and inspection efforts. Powder metallurgy processing programs should significantly reduce both the amount of raw material and the machining effort required for compressor and turbine disks. The number of fabricated engine-cases can be reduced by incorporating lower-cost cast cases using techniques under development. Similarly, the use of net shape extrusions and improvements in die casting techniques can reduce the number of forged parts rejected. Rotary forging efforts were projected to reduce shafting costs. Improved laser drilling techniques should significantly reduce the cost of producing small holes.

Acoustic Technology

The reduction of engine noise is in general accomplished at the expense of performance and weight. Because these penalties have been of major importance, the projections in the area of acoustics concern the technologies required to meet expected Federal Aviation Regulations on noise (FAR 36) with significant reductions in these penalties. The advanced technologies are expected to be realized from recent, current, and planned programs. Engine components will be designed to have lower inherent noise levels than heretofore. Better acoustic treatments and the ability to satisfy many structural requirements with acoustic panels are also expected. Inlet rings or duct splitters would be required to adequately reduce fan noise if only current technology were to be used. However, advanced technology, special inlet contours may be capable of providing comparable benefits with a smaller penalty. Exhaust noise suppression devices can also be made significantly more effective through the application of advanced technologies.

Engine-Nacelle Integration Technology

The technologies projected for engine-nacelle integration are reduced structural weight and reduced aerodynamic flowfield losses. The projections are based on experimental programs and analytical design systems that predict three-dimensional flowfields, boattail separation criteria, and Reynolds number effects.

PROCEDURE

To provide the criteria for evaluating the various HP compressor configurations, the following figures-of-merit were selected.

Return-on-investment (ROI)
Direct-operating-cost (DOC)
Fuel-burned (FB)
Takeoff-gross-weight (TOGW)
Life-cycle-cost (LCC)
Number-of-parts (NOP)

The figures-of-merit (FOM's) are defined in the following section.

A matrix of 49 high-pressure compressors was developed by statistical techniques. These configurations were then processed through a P&WA Compressor Configuration Design System (meanline design system) from which compressor efficiency and geometry were obtained. Statistical analysis procedures (regression equations) were developed, and an analysis was performed on the efficiency data to determine both the compressor configuration with the optimum efficiency and the relative sensitivity of efficiency to design variables. Thirty-four compressors were selected from the 49 compressor matrix, and their primary FOM's were calculated. A regression analysis of the ROI data was performed to determine the compressor configuration with the maximum ROI. During the early screening processes, additional configurations were incorporated into the matrix, which improved the accuracy of the equations, primarily in the area of optimum configurations.

The high-pressure compressors with the best ROI were compared with the configurations that had optimum efficiency. From this comparison, three new designs predicted to be optimum were selected and processed through the Compressor Configuration Design System, and FOM's were calculated. The three selected high-pressure compressors were reviewed in detail with emphasis on structural acceptability, maintenance costs, and the compressor's interrelationship with other components

From the study of the three selected designs, two new configurations meeting all structural requirements were selected. These two selected configurations were processed through a streamline analysis design program in which turbine cooling and customer bleed requirements were taken into account. The two configurations also underwent a further review in which maintenance costs and technology development risks were considered. On the basis of this evaluation and the calculated ROI, the optimum high-pressure compressor configuration was selected.

The overall plan utilized in the program is shown in the flow diagram presented in Figure 5.

FIGURES-OF-MERIT AND TRADE FACTOR APPROACH

Return-on-investment for an aircraft, based on the discounted cash flow method, is defined by

$$ROI = \frac{\text{Cash Flow}}{\text{Investment}} \times \frac{(1 + ROI)^N - 1}{(1 + ROI)^N}$$

where

Cash Flow	=	Revenue – Direct Operating Cost – Indirect Operating Cost – Taxes + Depreciation
Investment	=	Airframe Price + Engine Price + Airframe Spares + Engine Spares
N	=	Life of the Investment, years

Direct-operating-cost for an aircraft is a summation of crew costs, fuel costs, airframe and engine maintenance costs, insurance costs, and costs associated with depreciation and overhead (burden). Crew costs (flight deck only) are a function of aircraft productivity and weight. Fuel costs are influenced by aircraft drag and engine thrust-specific-fuel-consumption. Aircraft size and component prices affect airframe maintenance costs. Engine maintenance costs are functions of engine complexity, life of parts, and spare-part prices. Insurance and depreciation costs are both related to total aircraft prices. Overhead costs are proportional to maintenance labor requirements.

Direct-operating-cost plus interest adds to DOC the cost of capital (i.e., the interest paid by an airline on its investment)

Fuel-burned is the net fuel consumed by the aircraft during its mission. In general, takeoff, climb, acceleration, cruise, and descent are the mission elements considered. Fuel-burned is affected by the engine thrust-specific-fuel-consumption and the aircraft drag, weight, and size.

Takeoff-gross-weight is the gross weight of an aircraft prepared to takeoff on its design mission at its design payload. It is comprised of aircraft empty weight, payload, and fuel weight.

Life-cycle-cost is the total operating cost of an aircraft over its economic life, including investment, direct operating costs, indirect operating costs.

Number-of-parts of an engine is often considered a FOM because it is an indicator of the purchase price level and the cost to maintain the engine.

The effects on engine/aircraft system performance of variations in engine components were calculated in terms of several of the figures-of-merit. The purpose of this first calculation was to select the optimum values of the compressor design variables and to provide the capability for evaluating the relative sensitivities of the various inputs in order to increase technical insight as to the best areas for compressor advancement.

To calculate these FOM's, a method was used which is relatively facile and yet sufficiently sensitive to evaluate small changes. The method employed trade factors or partial derivatives established through the use of the model depicted in Figure 6. Trade factors were established for each engine characteristic (thrust-specific-fuel-consumption, weight, price, dimensions, and maintenance cost; and each FOM under consideration by making small, independent changes to each engine characteristic (from the basepoint engine) and measuring the effect of the change on each FOM as calculated by the model. This process began with the input of aircraft configuration data, aerodynamic considerations, engine performance and weight, and aircraft operational requirements. An iteration within the system defined the aircraft required to accomplish the mission specified in the input. The characteristics of this aircraft were then passed on to the airframe pricing model. Airframe pricing output data were added and this result was used as input to the airline economics model where ROI, indirect-operating-cost, revenue, etc. were calculated. The related trade factors of the engine characteristic-FOM's were then calculated using the complete basepoint aircraft simulation as established.

ENGINE MAINTENANCE COST ASSUMPTIONS

Engine maintenance cost is a significant variable in the design and evaluation of an advanced engine and its components, and includes both material and labor. In general, maintenance cost estimates were based on data obtained from operating experience in inspecting, maintaining, and servicing engines as the engines accumulate operating time. With these data and a comparison of key technology-influenced design differences, service lives for the advanced technology components were predicted by adjusting the field experience based on average part-lives. Total-maintenance (material and labor) requirement differences were then determined, and a conversion to cost differences was made using spare-parts price differences and standard labor rates.

Information obtained during the NASA-sponsored American Airlines Study of the Economic Effects of Propulsion Technology on Existing and Future Transport Aircraft (ref. 3) was useful for identifying the impact of engine technological advancements on propulsion system maintenance cost. Two methods, a detailed "Long Form" and a less detailed "Short Form", had been developed for estimating maintenance cost of an engine. The Long Form method, a module-by-module analysis of removal rates and repair costs, requires a detailed description of the six major modules of the engine, including pressures, temperatures, diameters, tip speeds, stages, and spare-part prices. The complexity of the Long Form method precluded its use for quick approximations of basic engine maintenance cost levels. For quicker but less accurate maintenance cost estimates, the Short Form was used.

Since this earlier NASA study, P&WA has made several modifications to the Long Form method. These modifications allow for the proper reflection of advancements in engine maintance technology and performance retention capability. The modified Long Form methodology, presently in general use at P&WA for estimating costs in the more detailed advanced engine studies, was used in the latter process steps in selecting the optimum configuration.

PARAMETRIC ENGINE EVALUATION USING BASE ENGINE

An initial-screening, parametric curve procedure was used for rapid and economical evaluation

of the many high-pressure compressor designs obtained from the study matrix. The engine parametric curves defined were thrust-specific-fuel-consumption and engine diameter, length, weight, and price without including the length, weight, and price of the compressor. To develop the parametric curves, a range of possible compressor efficiencies, combustor pressure losses due to variations in compressor exit Mach number, and rotor speeds were established. These parameters were chosen as the independent variables because they are the principal effect-oriented engine parameters exclusive of actual compressor geometry. Based on the ranges established, a limited array of variations between hardpoint† engines and the base engines (STF 477) were evaluated to obtain the data with which to prepare the parametric curves.

First, the inputs required to perform the engine cycle performance variation and size scaling analyses were defined. Ranges of high-pressure compressor efficiency (from 80% to 92%) and exit Mach number (from 0.22 to 0.46) were established to cover the extremes anticipated for the defined study matrix. High-pressure compressor rotor speed levels were selected. The maximum rotor speed was based on projections of the turbine stress capability of the base engine; a seventeen percent lower speed was selected as the minimum to achieve the lowest desired compressor inlet tip speed. The selected compressor exit Mach number range was then converted to diffuser-burner pressure loss values based on the best combustor configuration projected at each Mach number level. A limited array of variations between specific hardpoint engines and the base engine was then selected, and pertinent data were used as input to the performance analyses.

Cycle variations to the base engine were calculated for each of the specific cases in the array using a P&WA computer system, "State-of-the Art Performance Program" (SOAPP). In performing these cycle analyses, only engine bypass ratio was varied while the base engine level of exhaust-nozzle/jet-velocity ratio was held constant at 0.74, a level which in previous studies provided a good trade between thrust-specific-fuel-consumption (TSFC) and engine size. In addition, all base engine component performance was held constant except for high-pressure compressor efficiency and combustor pressure loss which were varied as indicated in the hardpoint array. With each cycle variation defined, SOAPP analyses were used to determine engine thrust, TSFC, total fan airflow, and high-pressure and low-pressure turbine design requirements for each of the cases. A parametric curve for TSFC was prepared directly from these data. Based on the resulting thrust data, engine size scaling requirements were established to allow adjustment of the base engine components to the constant thrust size required by the selected base four-engine aircraft. A parametric curve for engine diameter was then prepared by applying the size scaling requirements directly to the base engine. The effects of efficiency on cruise TSFC and fan tip diameter are shown respectively in Figures 7 and 8.

To establish a base for preparing the other parametric curves (engine length, weight, and cost), variations between base and hardpoint component flowpaths were estimated for each selected hardpoint case. The flowpaths were estimated from the cycle, and performance was derived from each case. Specifically, the base engine fan section was scaled to reflect the effects of

† "Hardpoint" is a preliminary design of a complete engine which defines the engine's physical characteristics (i.e., diameter, length, and weight) and its price.

cycle bypass ratio and total airflow (thrust) size. Low-pressure compressor flowpaths were defined to provide the same mean wheel-speed in the adjusted airflow size as the base engine. The base engine high-pressure compressor and its lower rotor-speed version (two stages added) were scaled to the appropriate airflow sizes and evaluated for flowpath dimensional purposes, but these compressors were not included in subsequent engine weight and price estimates. Combustor flowpaths were then defined to provide the best overall performance as functions of high-pressure compressor exit Mach number, and size scaling data were calculated for them. Based on the high-pressure compressor work requirements and adjusted airflow sizes, the high-pressure turbine flowpaths were defined at approximately the load factor level of the base engine in order to keep their efficiencies constant. Similarly, the low-pressure turbine flowpaths were also defined at approximately the base-engine load factor level based on fan and low-pressure compressor work, airflow size, and high-pressure turbine requirements. Parametric curves of engine length without the high-pressure compressor were prepared directly from the flowpath data. Figure 9 presents characteristic curves showing relative engine length without HP compressor as functions of efficiency over a range of exit Mach numbers and inlet corrected specific flows.

To prepare the parametric engine weight and price curves, the components of each hardpoint engine, exclusive of the HP compressor, were weighed and costed based on the mechanical-structural base engine configuration. The weights and costs for those engine components that changed relative to the base engine (e.g., combustor and turbines) were obtained with an established computerized estimating technique which modifies demonstrated engine component designs to reflect differences in size, aspect ratios, number of stages, materials, speeds, temperatures, pressures, etc. For components which differed from the base component in size only (e.g., the fan), weight and cost scaling was done using techniques developed from previous detailed design engine component scaling efforts. The total weight and cost of the engine without the HP compressor was then obtained for each hardpoint. Costs thus obtained were converted to prices on the basis of financial considerations projected for the 1980's operational period. These data were used to prepare parametric curves of engine weight and price without the HP compressor included.

COMPRESSOR DESIGN APPROACH

HP Compressor Aerodynamic Requirements

The design point requirements of overall pressure ratio, flow capacity, efficiency, surge margin, RPM, and durability were established from base engine considerations. High-pressure compressor configurations that met these requirements were selected in a preliminary design phase that involved parametric configuration studies coupled with performance, weight, and manufacturing cost trades. The final HP compressor, in addition to satisfying design point requirements, had to provide adequate efficiency and surge margin over the operating range from start-up to maximum rotor speed.

Compressor Design Process

The high-pressure compressor design process consisted of two basic phases: (1) a parametric screening study phase which included a preliminary aerodynamic design involving *meanline* studies to optimize the HP compressor configuration and (2) an optimum configuration evaluation phase in which a detailed aerodynamic, *streamline* analysis design program was used to define blading. The detailed design program was only used for evaluating the final selected designs.

Preliminary Aerodynamic Design

The HP compressor configuration for a specific engine requirement was determined during the Preliminary Aerodynamic Design phase, using the P&WA Compressor Configuration Design System. This design system consists of a meanline analysis computer program in conjunction with empirical correlations of loading limits and changes in blade loadings as a function of surge margin. The meanline analysis computer program defined the HP compressor configuration and efficiency as functions of the HP compressor design parameters through an iteration process. The following HP compressor design parameters were varied in these studies: flowpath shape, hub-tip ratio, inlet specific flow, exit Mach number, degree of reaction, aspect ratio, solidity, and rotor speed. The design point conditions of inlet corrected flow, overall pressure ratio, required surge margin, and RPM were determined by the base engine requirements. The meanline analysis computer program calculated meanline velocity triangles by solution of the continuity and Euler equations, and determined losses for both the core flow and the endwall region (ref. 4). Since the loss correlations used in the program were representative of Reynolds numbers on the order of 10^6, a Reynolds number correction was made to the efficiency calculated from the loss system.

The Compressor Configuration Design System defined a flowpath, rotor speed, number of blades and vanes, blade and vane chords, and a first-pass compressor length for a given number of stages, with a resultant efficiency.

Detailed Aerodynamic Design

During this phase of the aerodynamic design process, the HP compressor flowfield was fully defined, initial blading was selected, and structural analysis iterations were performed.

The definition of the HP compressor flowfield was accomplished using a streamline analysis computer program to establish full-span aerodynamics. This streamline analysis program defined velocity vectors and flow conditions by means of an axisymmetric compressible flow solution of the continuity, energy, and radial eqilibrium equations. Streamline curvature, enthalpy, and entropy gradient terms were included in the equilibrium equation, as shown in Figure 10.

In the flowfield definition phase of the design process, initial flowpath calculating stations for streamline analysis had to be selected. The location of these stations was facilitated by the root, mean, and tip airfoil section definition and blade-row gapping estimates which were obtained from the Compressor Configuration Design System. Bleed locations were determined

(turbine cooling air, customer service air) and bleed flows accounted for in the flowfield definition. The effects of the boundary layer blockage on the flowfield were also accounted for. The initial choice of rotor pressure ratio and efficiency, stator loss and exit angle, and boundary layer blockages were based on the output from the Compressor Configuration Design System.

Using the streamline analysis program, the spanwise and stagewise loading distributions were optimized by adjustments in flowpath shape, radial total pressure slopes, axial pressure distributions, and radial reactions.

Once the flowfield aerodynamics had been optimized, preliminary blading was selected. Radial chord distributions (taper ratio) were selected to maintain loading limits where required. Blading in the subsonic Mach number region was selected using the P&WA cascade system which was incorporated in the streamline analysis program. For blading selection in the supersonic Mach number regime, correlations of loss and turning data acquired from extensive high tip speed fan tests were employed in conjunction with channel flow calculations to determine blade section shapes. The selected blading was subjected to structural analysis, and initial structural-aerodynamic compromises were made.

The streamline program, in conjunction with the P&WA cascade system, and correlations mentioned above were used to predict the performance and surge line over the expected range of operation of the IIP compressor. This predicted off-design HP compressor performance was used on an engine matching computer program to define the HP compressor operating line at off-design conditions.

Distributions of Independent Compressor Parameters

Certain assumptions of axial distributions of independent compressor parameters were used in the Compressor Configuration Design System which produced the input to a regression analysis for optimizing efficiency. The average levels of these parameters were permitted to vary over a range determined from the statistically designed matrix of parameter ranges, while the distributions followed the forms described below.

The level of stage reaction was held constant throughout the compressor and resulted in an exit air-angle that generally was not axial. The exit angle was brought back to axial during the detailed design phase.

The distribution in axial velocity was linear throughout the compressor with inlet and exit levels determined by the range of parameters within the matrix. Inlet axial velocity was a function of the inlet specific flow selected for the configuration under study, and the exit axial velocity was a function of the selected exit Mach number.

Solidity distribution was maintained constant throughout the compressor except for the higher tip speed rotors where tip solidity was varied for optimum performance as functions of tip speed and inlet hub-tip ratio. Conventional fan design techniques for MCA airfoil sections at transonic and supersonic blade Mach numbers were used to derive these solidity trends for the high tip-speed rotors.

An axial distribution of aspect ratio was prescribed by structural considerations for a compressor of moderate to high average aspect ratio. This distribution was modified for other levels of average aspect ratio by direct scaling of each local value with the average. Structural considerations included torsional flutter limits in all stages and margin from 2E (2 exitation per revolution) resonance in a shroudless first stage.

STATISTICAL ANALYSIS FOR ECONOMIC AND HP COMPRESSOR EFFICIENCY EVALUATION

The Compressor Configuration Design System was used to define the configuration and efficiency for each of the 49 compressors contained within the statistically designed matrix (Figure 11). All 49 compressors were designed for an 18:1 pressure ratio with loading levels consistent with a 15 percent surge margin at the aerodynamic design point (ADP) and with an average running tip clearance of 0.254 mm [0.010 in.]. A mathematical regression analysis was performed on the efficiency data to determine the HP compressor configurations that yielded optimum efficiency and also the relative sensitivity of efficiency to the parametric design variables.

The compressor design parameters selected as independent variables for exercising the 1985 technology were:

- Rotor speed (rpm)
- Flowpath Geometry (COD, CMD, CID)
- Inlet Hub-Tip Ratio (H/T)
- Inlet Specific Flow (W/A)
- Exit Mach Number (M_{NE})
- Reaction (Average)
- Blade Aspect Ratio (Average)
- Solidity (Average)
- Number of Stages (6 to 12)

The initial step in the evaluation process was to define the configuration matrix for the study. A statistically designed matrix approach was used based on the premise that combined responses due to simultaneous changes in two or more design parameters are important. And a statistical approach is the most efficient and economical way to obtain information on the effects of these responses. An engineering approach without the assessment of these effects would have made the selection of the optimum HP compressor much more difficult, considering the prodigious number of possible combinations.

The range of variables chosen for the initial screening was:

COMPRESSOR DESIGN PARAMETERS	RANGES INVESTIGATED				
Speed (rpm)	16350		18025		19700
Flowpath	CID		COD		CMD
H/T Inlet	.45	.50	.55	.60	.70
Exit Mach No.	.22	.26	.30	.38	.48
Aspect Ratio (av)	.8	1.0	1.2	1.6	2.0
Reaction (av)	.50	.55	.60	.70	.80
W/A (kg/sec-m^2)	166	176	186	195	205
[lbm/sec-ft^2]	34	36	38	40	42
Solidity (av)	.8	.9	1.0	1.1	1.2

The statistically designed matrix was a Box-Wilson design (Figure 11), typically utilized for optimization studies. Although forty-nine compressors were investigated initially, an additional 16 configurations were added later to permit development of more accurate mathematical models. Using the results of the Compressor Configuration Design System as input, a statistical evaluation was performed to predict efficiency and number-of-stages as functions of the design parameters. These models were developed by the least-squares curve fitting techniques (regression analysis). The resulting mathematical functions had the following form:

$$\left.\begin{array}{l}\text{Efficiency (HPC)}\\ \text{or}\\ \text{Number of Stages}\end{array}\right\} = f(\text{Compressor Design Parameters})$$

$$\left.\begin{array}{l}\text{Efficiency (HPC)}\\ \text{or}\\ \text{Number of Stages}\end{array}\right\} = a_o + a_1 \times \text{speed} + a_2 \times \text{flowpath} + \ldots + a_8 \text{ gap chord} + b_1 (\text{speed})^2 + \ldots + b_8 (\text{gap chord})^2 + c_{1\text{-}2} (\text{speed} \times \text{flowpath}) + c_{1\text{-}3} (\text{speed} \times \text{inlet hub-tip ratio}) + \ldots + c_{7\text{-}8} (\text{specific flow} \times \text{gap chord})$$

Where gap chord is the reciprical of solidity, and a_o, a_n's, b_n's, and $c_{n\text{-}j}$'s are coefficients calculated by regression analysis.

The calculation of the regression coefficients was developed with an available computer program with interactive and graphical analysis by light pen and scope system.

The accuracy factor for a regression model is called the Standard Error Estimate (SEE) and is defined as

$$SEE = \sqrt{\frac{\sum_{i=1}^{i=n} (\eta_{given} - \eta_{predicted})}{n - K}}$$

Where

η = efficiency

n = number of compressor configurations studied

K is the number of coefficients (a, b, and c's) estimated.

An acceptable regression model was developed for η_{HPC} with the accuracy factor (SEE) being).44%.

Next, a least-square regression model was developed to predict number-of-stages as a function of the compressor design parameters. This model was also complex in nature and was dependent only on the original eight compressor design parameters. The calculated accuracy factor for this model was ±0.39 stages which is considered acceptable. The same method as used for compressor efficiency was employed to establish the validity of the regression model. It was checked against the calculated number of stages from the meanline computer decks, with excellent agreement.

After establishing the capability of predicting both the HP compressor efficiency and number of stages, a computer optimization program was developed to establish the optimum efficiency of the compressor for a given number of stages.

PARAMETRIC EVALUATION OF HP COMPRESSOR FOR INSERTION INTO ECONOMIC FOM REGRESSION ANALYSIS

To estimate a total engine length, weight, and price for the FOM analyses, 34 of the 49 high-pressure compressors defined in Figure 11 were analyzed further. These compressors had previously been aerodynamically and geometrically defined in the base engine airflow size. The data from these compressors were now used as input into computerized component programs. Weight and cost estimates were made for each in the base engine airflow size. With base geometries, weights, and costs thus determined for all the high-pressure compressors in the matrix, each compressor was integrated into its variation of the base study engine. The first step in this integration was to adjust the size, weight, and cost of each compressor based

on the value indicated from the parametric size-scaling data. These adjustments were made using techniques developed during previous compressor scaling efforts. Next, the immediate interfaces of each compressor (the fan-compressor transition duct, intermediate case, diffuser case, and combustor) were adjusted to ensure dimensional compatibility with compressor geometry. The effects of the resulting changes on weight and cost were then estimated. These weight and cost differences, along with the length effects determined in the integration, were combined with the previously estimated compressor weight, cost, and length to arrive at the total compressor impact on the engine. Resulting compressor costs were then converted to prices using the factor projected for the rest of the engine.

Total engine weight, price, dimensions, and performance for each of the 34 FOM matrix cases were then calculated. Total engine weight and price were determined by combining the engine values without the compressor from the parametric weight and price curves with the total compressor value estimated. Engine TSFC and fan tip diameter were obtained from the parametric performance and dimension curves. Final engine lengths were estimated by combining the values of engine length without the compressor (obtained from the parametric dimension curve) with the estimated length of the total compressor. This portion of the study procedure provided a total engine weight, price, length, diameter, and TSFC for each FOM matrix compressor. In each case, the engine reflected the proper bypass ratio cycle variation and the thrust size required by the airplane.

The final step in this process was to determine the FOM's for each of the 34 matrix cases. First, the total engine weight, price, performance, and dimensional data determined for each matrix case were converted to differences (Δ's) relative to the base engine values. Next, maintenance cost changes relative to the base engine were approximated using the Short Form Method. The established trade factors were used to calculate the FOM's for each matrix case. This calculation determined the separate contribution of each FOM input (e.g., ΔROI weight, ΔROI TSFC, ΔROI price). These individual effects were then combined to form the final FOM (e.g., ΔROI). Final FOM's thus determined were the inputs to the FOM regression analyses.

Establish Figures-of-Merit Variation With Number-of-Stages

The following mathematical models, other than compressor efficiency, were developed for FOM's:

Return-on-Investment (ROI)
Fuel-Burned (FB)
Direct-Operating-Cost (DOC)
Takeoff-Gross-Weight (TOGW)

Least-squares regression analyses, as described for the HP compressor efficiency model, were utilized to predict the FOM's as independent compressor design variables.

The resultant models and accuracies were:

FIGURE-OF-MERIT	ACCURACY FACTOR
ROI	0.054
Fuel Burned	0.410%
DOC	0.005%
TOGW	61.95 kg [136.6 lbm]

These regression models were incorporated into the computer optimization program to search for the maximum FOM as a function of the compressor design parameters for a given number of stages.

SELECTION OF OPTIMUM CONFIGURATIONS

Three Best HP Compressor Configurations

Before the selection of the three best compressors, a group of 13 compressors were subjected to a preliminary mechanical design and structural review. The 13 compressors were chosen to cover a range of mechanical variations based on the FOM's obtained from the inital regression analysis models. These compressors had been aerodynamically and geometrically defined with the Compressor Configuration Design System; integrated into their respective variations of the base engine; and weighed, priced, and dimensioned. Total engine weights, prices, dimensions, and performances were then calculated. Figures-of-merit, including the Short Form maintenance costs, were also calculated and subsequently used to refine the FOM regression models. The mechanical design and structural review yielded estimates of stiff-bearing critical speed; 1st-stage rotor blade resonance margin; 1st-stage rotor disk size; flutter stability of front, middle, and rear stages; and flowpath impact on adjacent structures.

The review to which these 13 compressors were subjected was undertaken to provide structural criteria for determining the three best HP compressors. Structural constraints had not been previously imposed on the selection process. Selection of the three best compressors, however, was not restricted to the 13-compressor group.

Two Optimum HP Compressor Configurations

The three best configurations selected previously were reviewed in greater depth, and first-pass blade shapes were obtained for the front, middle, and rear stages. A structural analysis, more comprehensive than before, was also performed to determine resonance and flutter margins. As a result, more specific structural guidelines were obtained. In addition, return-on-investment was recalculated to include the modified Long Form maintenance-materials-cost estimate. The two optimum compressor configurations were then selected. This selection was not necessarily limited to the three previously chosen configurations.

Selection of the Optimum HP Compressor

The final selection of the optimum HP compressor was based on streamline analysis of the two optimum HP compressors, including the effects of turbine cooling bleed and customer service bleed. Previous selections were based on a meanline analysis, the Compressor Configuration Design System.

In the streamline design analysis process, the initial flowpath calculating stations and other input were taken from a meanline analysis that had previously been performed. Flowpath was then adjusted at the ID to account for interstage bleed flows used for turbine cooling air and customer service air. The flowpath adjustments were required to reduce flow areas to maintain Mach numbers downstream of the bleeds. This adjustment increased exit hub-tip ratios.

Stagewise and spanwise loading and incidence distributions were optimized through adjustments in stage pressure ratio and reaction and in radial total pressure and reaction. Airfoil geometry was selected by methods appropriate to subsonic or supersonic Mach number regimes. Structural analysis of the blading included a review of stresses, blade resonance modes, and flutter stability. Maintenance cost estimates were made using the modified Long Form method. Resulting total engine weight, price, dimensions, performance, and maintenance costs were then used as input to the FOM analyses.

RESULTS AND DISCUSSION

PARAMETRIC SCREENING STUDIES

High-Pressure Compressor Efficiciency

The regression models developed for HP compressor efficiency and number of stages agreed closely with the meanline configuration design system (within the standard error of estimate noted in the section "Statistical Analysis for Economic and HP Compressor Efficiency Evaluation". Because of the complexity of the regression model in which interactions between design variables play a major part, the trends of HP compressor efficiency with the eight independent compressor design parameters are difficult to describe graphically. Rather than provide curves from the regression model, trend curves for each variable were derived from the meanline system. These trends are shown in Figure 12.

The peak efficiency HP compressors from the regression model were obtained from a computer-optimization program developed to search for the optimum compressor configuration within specified limits of the independent compressor design parameters. The result of this search is presented in Figure 13, which shows the relative adiabatic efficiency trend with number of stages. The optimum 12-stage compressor has the highest efficiency because the trend to lower rotor speed and lower specific flow with increased number-of-stages reduces airfoil losses and thus increases efficiency. Efficiency, however, was only one of the inputs to the FOM. The best FOM configurations generally were not the configurations showing best efficiency.

Engine System Figure-of-Merit Evaluation

Regression models for ROI, FB, DOC, and TOGW were searched with a computer optimization program for optimum FOM's as functions of compressor design parameters for a given number of stages. No structural constraints were imposed on the search of initial FOM models other than limiting the inlet hub-tip ratio to a minimum of 0.50 and the exit hub-tip ratio to a maximum of 0.96.

Figure 14 shows the results for ΔROI (change in return-on-investment). Trend curves that reflect the Short Form maintenance cost approach show that maximum ΔROI would be achieved with a 9 stage design (Figure 14).

The general trend of ΔROI with number of compressor stages was influenced most strongly by either the trend of TSFC or compressor efficiency. For configurations with fewer stages, a TSFC penalty combined with a small increase in engine weight overpowered the price and maintenance cost improvements. For configurations with a greater number of stages, TSFC was essentially an invariant, and the increasing propulsion system drag associated with the longer engine became an influencing factor in reducing ΔROI.

The ΔFB (change in fuel burned) results are presented in Figure 15 which shows minimum ΔFB occurring with 11 to 12 stages. As was the case for ΔROI, the general trend of ΔFB with number of stages was influenced most strongly by the trend of TSFC. For configurations with fewer stage numbers, a TSFC penalty combined with a small weight penalty to increase ΔFB. The TSFC for configurations with a greater number of stages was again almost constant and increasing drag became an influencing factor.

Figure 16 shows the trend ΔDOC (change in direct-operating cost) with number of stages. In general, the ΔDOC results were similar to those for ΔROI, and for the same reasons.

The ΔTOGW (change in takeoff-gross-weight) trend with number of stages is presented in Figure 17. In general ΔTOGW trends were similar to those for ΔFB, with minimum ΔTOGW occurring with 9 stages. The trend of ΔTOGW with number of stages was influenced most strongly by the TSFC trend although propulsion system weight was of some importance. For configurations with fewer stages, higher TSFC and slightly higher weight combined to increase ΔTOGW significantly. For the configurations with the higher number of stages, the almost constant TSFC and small weight change did not significantly affect ΔTOGW, and the increased drag became the governing factor.

SELECTION AND EVALUATION OF OPTIMUM HP COMPRESSORS

Three Best HP Compressors

The search for an optimum ROI configuration yielded definite HP compressor characteristics. The analysis also revealed many configurations that could be selected within the known error tolerance band for the ROI regression model equation.

The meanline analysis and hardpoint calculations determined the accuracy of the regression equations for both HP compressor efficiency and FOM models, as shown below, for an 8-stage compressor.

	REGRESSION	HARDPOINT
Tip Speed, m/sec [ft/sec]	463.3 [1520]	463.3 [1520]
Inlet Hub-Tip Ratio	0.575	0.577
Aspect Ratio (av)	1.2	1.2
Efficiency (adia.)	0.8796	0.8786
Δ ROI	+0.0610	+0.0620
Δ DOC (%)	−0.1538	−0.1519
Δ FB (%)	−0.362	−0.168

The thirteen hardpoint configurations were added to the FOM regression models, and a new equation was derived with improved accuracy, particularly in the area of interest for the optimum ROI compressor selection.

The structural review of the 13-compressor group established the following initial structural constraints:

- Corrected tip speed below 472.4 m/sec [1550 ft/sec] should aid in avoiding a 1st-stage rotor 2E (excitations per revolution) resonance.
- A combination of low first-stage aspect ratio (average aspect ratio below 1.3) and inlet hub-tip ratio greater than 0.55 should provide adequate 2E resonance margin for the first blade and low-cycle-fatigue life for the first disk.
- Average aspect ratios less than about 1.3 should avoid a middle-stage flutter stability boundary.
- A rotor stack having a length-to-diameter ratio of less than approximately 2.5 should avoid critical speeds in the operating range and should be sufficiently stiff to permit tight blade tip clearance control.
- Exit hub-tip ratios less than 0.94 should provide practical tip-clearance control.

From this understanding of structural constraints and optimum FOM's, a tighter design parameter mesh was chosen and used in a second FOM search for compressors having optimum ROI and FB. The restricted ranges of parameters were, for example, as follows:

Inlet hub-tip ratio	0.57, 0.58, 0.59, 0.60, 0.61, 0.62
Exit Mach Number	0.25, 0.275, 0.30, 0.325, 0.35, 0.375
Aspect Ratio (avg.)	1.0, 1.1, 1.2, 1.3, 1.4
Inlet Specific Flow	39, 40

The results of the search are shown in Figures 18 and 19 for ΔROI and ΔFB, respectively. The ΔROI trend was not changed by the structural constraints, but the level was slightly reduced, resulting in optimum compressors of 8 to 10 stages. The trend for ΔFB, however, reached an essentially constant value at 9 stages, and any further increases in the number of stages no longer indicated any benefit.

These studies led to the selection of the 8-stage, 9-stage, and 10-stage compressors as the three best configurations. The selection was based primarily on optimum ROI and the need for a range in the number of stages to provide a variation in pressure ratio per stage, a measure of the degree of aggressiveness. The design parameters of the three configurations are:

No. Stages	8	9	10
Tip Speed (m/sec)	463.3	473.0	462.7
[ft/sec]	1520	1552	1518
Hub-Tip Ratio (inlet)	0.577	0.602	0.577
Hub-Tip Ratio (exit)	0.92	0.89	0.88
Exit Mach Number	0.31	0.26	0.26
Specific Flow	40	40	40
Aspect Ratio (av)	1.2	1.1	1.3
Solidity (av)	1.15	1.05	1.10
No. of Blades & Vanes	794	672	840
1st Rotor Press. Ratio	1.839	1.829	1.739
Efficiency, adia. (%)	87.9	88.0	88.4

Selection of Two Compressors for Preliminary Design

The three previously selected configurations were processed in greater depth to verify the original estimates of the broad structural constraints. In addition, maintenance-material-cost (MMC) were also recalculated. The more detailed modified Long Form was utilized, and the ROI figures-of-merit were recalculated to include the Long Form results.

Adjustment to the ΔROI to reflect the modified Long Form results shifted the peak ΔROI from the 9-stage to the 8-stage design as shown in Figure 20. As a result, an 8-stage compressor was one of the two configurations selected for the preliminary design. This shift in peak occurred because the trend toward fewer stages and lower aspect ratio (number-of-parts) benefitted the performance retention aspect of maintenance cost.

The three selected configurations (i.e., the 8-stage, 9-stage, and 10-stage designs) were reviewed in more detail to obtain approximate airfoil definition. To obtain resonance and flutter values, the first and last stages were again analyzed. This analysis more accurately defined the restrictions of inlet hub-tip ratio and 1st-stage rotor aspect ratio. The structurally acceptable region for first-stage resonance and allowable commercial LCF life is shown in Figure 21 with respect to aspect ratio, inlet hub-tip ratio, and tip speed. The figure shows that to satisfy the criteria for a disk LCF life of 12,000 cycles and a blade 2E resonance margin of five percent over the maximum rpm for the design tip speed (462.8 m/sec [1518 ft/sec]) of the optimum FOM configurations, the inlet hub-tip ratio cannot be less than about 0.57. This constraint was applied to all configuration choices regardless of number of stages.

Other constraints on the selection of two compressors for detailed preliminary design were apparent. Figure 22 indicates that even good clearance control and minimum running clearances of 0.254 mm [0.010 in.] do not permit selecting compressors of less than seven stages because the short blade-heights and large clearance-to-height ratios in rear stages would penalize HP compressor efficiency and TSFC.

A nine-stage configuration would normally have been selected as the other choice for the preliminary design since it ranked next to the eight-stage for optimum ROI. However, the NASA "Request for Proposals" upon which the subject contract was awarded suggested use of a pressure ratio per stage criteria as a measure of selection of the optimum configuration. Therefore, because of the significant improvement in pressure ratio per stage and the need to determine if any serious limitations would be exposed in a detail analysis, a 7-stage was selected as the other choice instead of a 9-stage. The average pressure ratio per stage for the 7-stage, 8-stage, and 9-stage designs are respectively, 1.51, 1.43, and 1.38 for an 18:1 pressure ratio compressor.

To select the two compressors for the preliminary design, the mesh size on the input parameters to the FOM regression analysis were further refined. This was done to provide a group of 7-stage and 8-stage configurations that meet the new structural constraints.

The mesh restricted the following parameters:

Aspect Ratio (average)	1.1, 1.15, 1.20, 1.25, 1.30, 1.35
Inlet Hub-Tip Ratio	0.58, 0.59, 0.60
Inlet Specific Flow	40

The regression analysis search for the optimum ROI configuration was completed, and the 7-stage and 8-stage configurations were chosen.

The hub-tip ratios and 1st-stage rotor aspect ratios of the two selected configurations were identical because both the 7-stage and 8-stage designs have the same rpm. This is the minimum hub-tip ratio allowed for the selected 1st-stage rotor aspect ratio. The 1st-stage rotor aspect ratio with the assumed aspect ratio axial distribution was predicted to be the optimum ROI configuration for the 7-stage and 8-stage compressors.

The selected optimum 7-stage and 8-stage compressors are compared below. The two compressors differ only in the trends toward reduced exit hub-tip ratio and solidity with increased number-of-stages.

No. of Stages	7	8
$U_{T, CORR}$ (m/sec)	465.7	465.7
[ft/sec]	1528	1528
H/T_{inlet}	0.58	0.58
H/T_{exit}	0.935	0.918
M_{NE}	0.35	[illegible]0
Aspect Ratio (av)	1.15	[illegible]15
W/A ($kg/sec\text{-}m^2$)	195	195
[$lbm/sec\text{-}ft^2$]	40	40
Flowpath Shape	CMD	CMD
Solidity (av)	1.21	1.13
Reaction (av)	0.52	0.51
Efficiency (adia.)	0.872	0.879
1st-Stage Pressure Ratio	1.90	1.85
Number of Blades & Vanes	781	746

Evaluation of Two HP Compressors

The selected 7-stage and 8-stage compressors were subjected to a complete compressor aerodynamic and structural design review, and turbine cooling and customer bleed requirements were included for the first time. As a result, exit hub-tip ratios were increased as shown below.

	EXIT H/T RATIO	
	7-STAGE	8-STAGE
Without bleeds	0.935	0.918
With bleeds	0.939	0.923

Both selected compressors were evaluated as to total impact on the base engine with respect to TSFC, weight, price, dimensions, and maintenance costs. The impact on the 7-stage compressor engine relative to the 8-stage is shown below.

Price	−0.28%
Length	−1.61%
Diameter (fan)	−0.08%
Cruise TSFC	+0.50%
Weight	+0.23%
Maintenance Cost	+0.14 $/EOH
Cruise Thrust	Same

The 7-stage compressor engine by virtue of its one less compressor stage is lower in price and shorter in length than the 8-stage engine. The 7-stage compressor, however, is less efficient than the 8-stage compressor and has a higher exit Mach number with a consequently higher combustor pressure loss, resulting in a higher engine TSFC and necessitating larger-diameter engine components (except for the fan). Although the impetus of one less compressor stage on engine price is sufficient to offset the contrary trend due to the increase in diameters, the larger diameters increase the aggregate weight of the engine and the cost of individual parts, especially in the hot sections of the engine. Since the hot sections are the inveterate high maintenance sections, maintenance costs are greater. The optimum by-pass ratio of the 7-stage compressor engine, because of the lower efficiency and higher pressure loss, is less than that of the 8-stage configuration, slightly reducing fan diameter.

Selection of the Optimum Configuration

The two chosen compressors were evaluated in terms of changes in return-on-investment, fuel-burned, direct-operating-cost, takeoff-gross-weight, and number-of-parts. The values of the 7-stage compressor engine FOM's relative to the 8-stage compressor engine are:

Return-on-Investment	−0.059
Fuel Burned	+0.637%
Direct-Operating Cost	+0.261%
Takeoff-Gross-Weight	+414 kg [913 lbm]
Number of Compressor Airfoils	+35

The 7-stage compressor engine is inferior to the 8-stage in all FOM's. The magnitude of the difference for ROI, the primary FOM, is equivalent to a change of about 0.4% in TSFC. The poorer ROI and FB values of the 7-stage compressor engine are primarily a result of higher TSFC. Higher TSFC and maintenance cost more than offset price advantage, causing the higher DOC. The TOGW penalty resulted from high TSFC and weight. The number-of-parts are greater for the 7-stage because solidity is higher. From this comparison, the 8-stage compressor was selected as the optimum configuration. A cross-section drawing of the optimum 8-stage compressor is presented in Figure 23.

The aggressive technology projections made for 1985 led to a significantly improved compressor design which requires fewer stages and parts while yielding a higher airline return-on-investment and a reduction in fuel-burned. Maintenance costs and airfoil-deterioration-life significantly influenced system economics. The optimum configuration, which has a comparatively low aspect ratio, is attractive both for performance and for system economics. The study further revealed that the most efficient compressor is not the optimum configuration when evaluated with respect to system economic factors.

Some important features of the optimum high-pressure compressor are:

Number of Stages	8
Tip Speed	465.7 m/sec [1528 ft/sec]
Inlet Hub-Tip Ratio	0.58
Exit Hub-Tip Ratio	0.923
Exit Mach Number	0.30
Aspect Ratio (av)	1.15
Specific Flow	197 kg/sec-m^2 [40.4 lbm/sec ft^2]
Solidity (av)	1.13
Reaction (av)	0.51
Number of Blades and Vanes	746
Efficiency (adia.)	87.9%

Stagewise rotor and stator plots of aerodynamic parameters are shown in Figure 24; mean-line results are included for comparison.

Rotor and blading aspect ratios:

STAGE NO.	ROTOR	STATOR
1	1.52	1.51
2	1.49	1.45
3	1.40	1.35
4	1.28	1.21
5	1.13	1.04
6	0.97	0.91
7	0.85	0.80
8	0.76	0.73 (double row)

The bleed flows and locations are:

TYPE	BLEED OFF STAGE LOCATION	BLEED FLOW (%)
Customer Bleed		
OD	6	4.1
Turbine Bleed		
OD	6	2.6
ID	4	1.0

Campbell diagrams for the first-stage and eighth-stage rotor blades are presented in Figure 25 and 26 respectively, and a summary of the structural analysis results are presented below.

- Rotor 1 2E Margin (Coupled) — 3.0% over maximum mechanical speed (21,500 rpm)
- 8th-Stage Rotor 1st Tip Mode Vane Passing Resonance Speed — 13,400 rpm (56E)
- Flutter Stability
  - Rotor & Stator — 1st- and 8th-stages acceptable margin
- Airfoil Root Static Stress
  - Rotor 1 (unconcentrated) — 557.2 X 10^6 N/m^2 [80.2 X 10^3 lbf/in^2]
  - Rotor 8 (unconcentrated) — 99.34 X 10^6 N/m^2 [14.3 X 10^3 lbf/in^2]
- Disk Bore LCF Life
  - Rotor 1 — 10^5 cycles
  - Rotor 8 — 10^4 cycles
- Disk Rim LCF Life
  - Rotor 1 — 10^4 cycles
  - Rotor 8 — 10^4 cycles
- Disk Burst Margin
  - Rotor 1 — 18%
  - Rotor 8 — 41%
- Disk Material
  - Rotor 1 — Improved Ti alloy
  - Rotor 8 — Improved IN-100

REFERENCES

1 Gray, D. E.: "Study of Turbofan Engines Designed for Low Energy Consumption, Final Report", NASA CR-135002, PWA-5318, 1976.

2 Bisset, J. W.: "Cost Benefit Study of Advanced Material Technologies for Aircraft Turbine Engines", NASA CR-134701. PWA-5073, 1974.

3 Sallee, G. P.: "Economic Effects of Propulsion System Technology", NASA CR-134645, 1974.

4 Hanley, W. T.: "A Correlation of Endwall Losses In Plane Compressor Cascades", *Journal of Engineering, for Power,* ASME, July 1968.

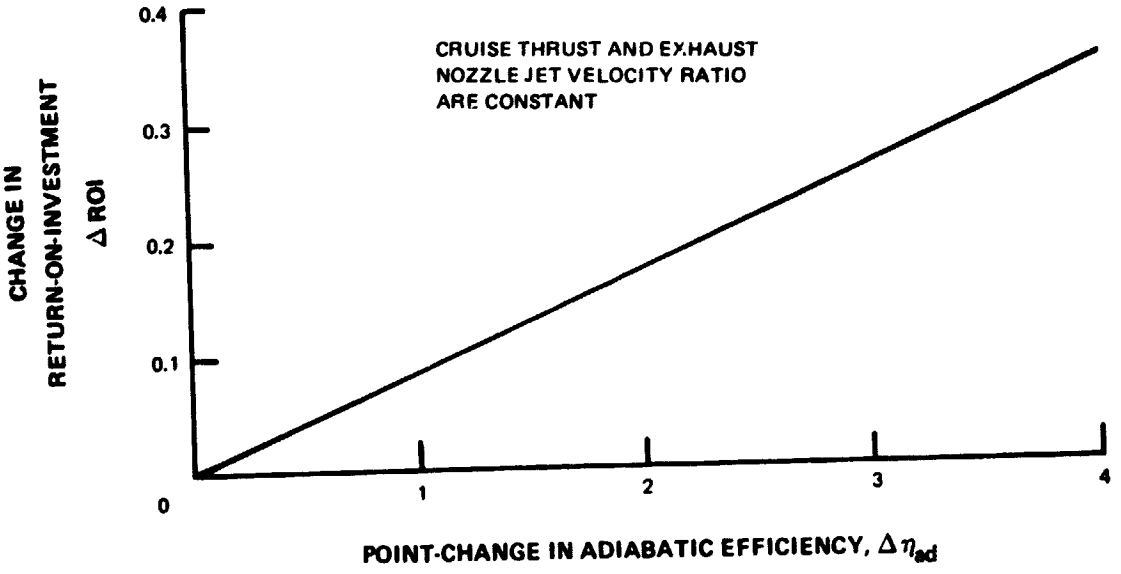

Figure 1 Effects of HP Compressor Adiabatic Efficiency on Return-On-Investment

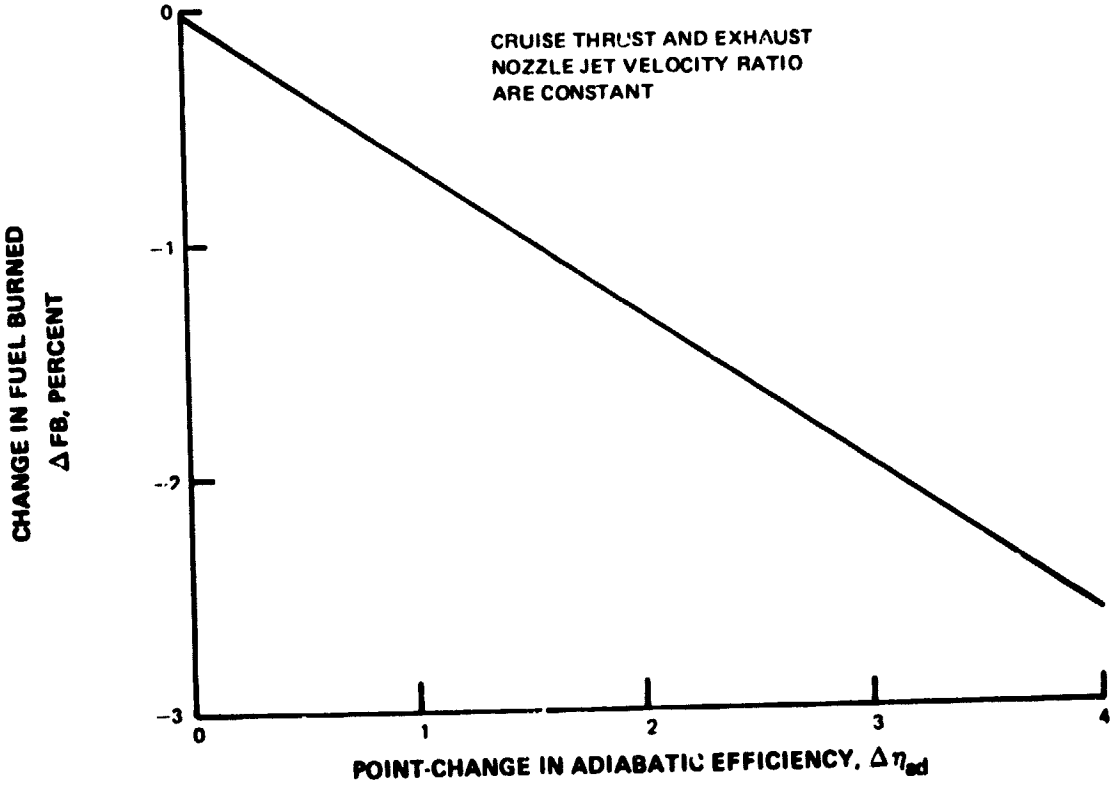

Figure 2 Effects of HP Compressor Adiabatic Efficiency on Fuel Burned

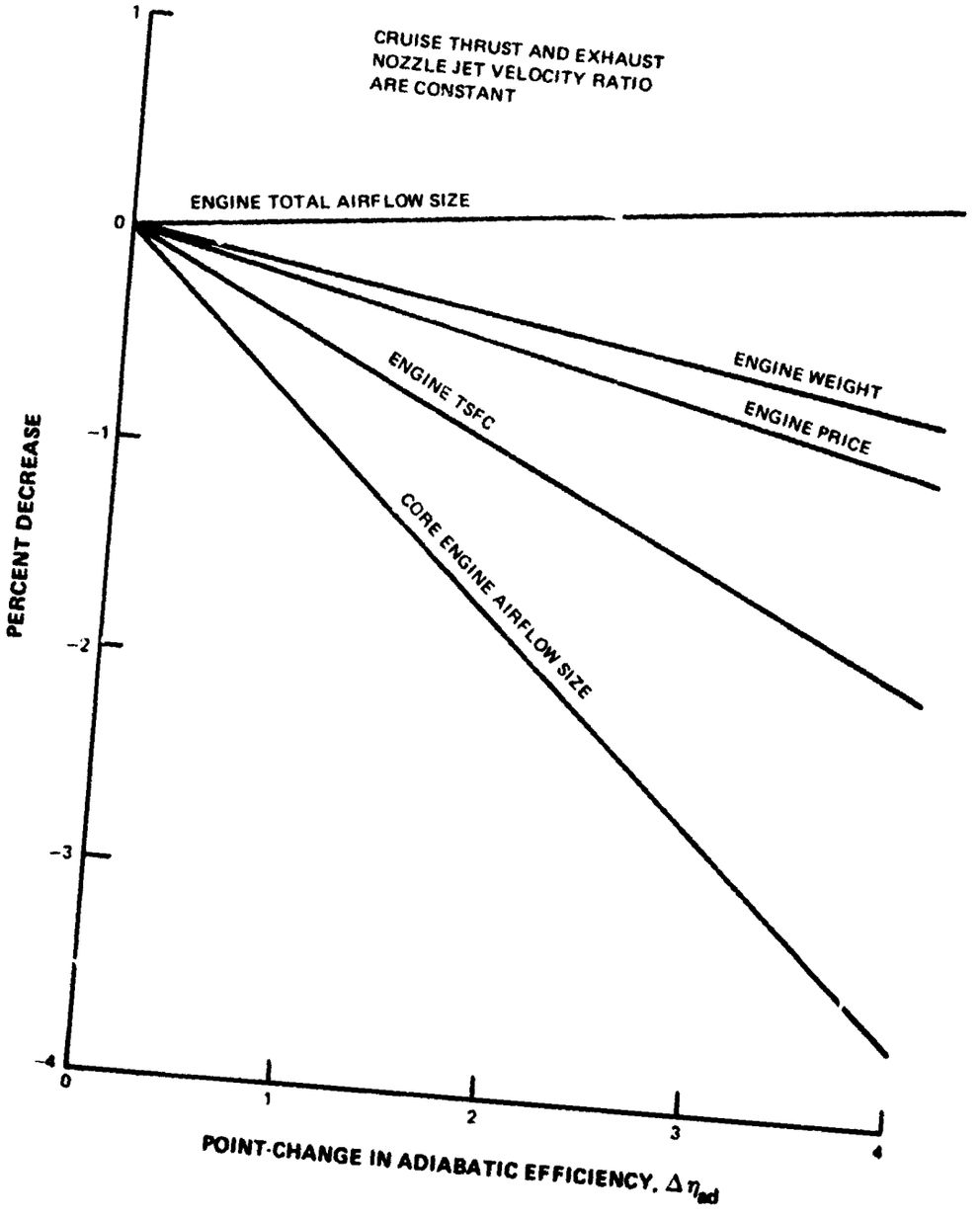

Figure 3 Effects of HP Compressor Adiabatic Efficiency on Engine TSFC, Airflow, Weight, and Price

SELECTED CYCLE

- 1470°C [2600°F] COMBUSTOR EXIT TEMP
- 45 1 PRESSURE RATIO
- 8.0 BYPASS RATIO
- 1.7 FAN PRESSURE RATIO

18·1 HIGH PRESSURE COMPRESSOR
24.3 kg/sec [53.6 lbm/sec] CORRECTED AIRFLOW

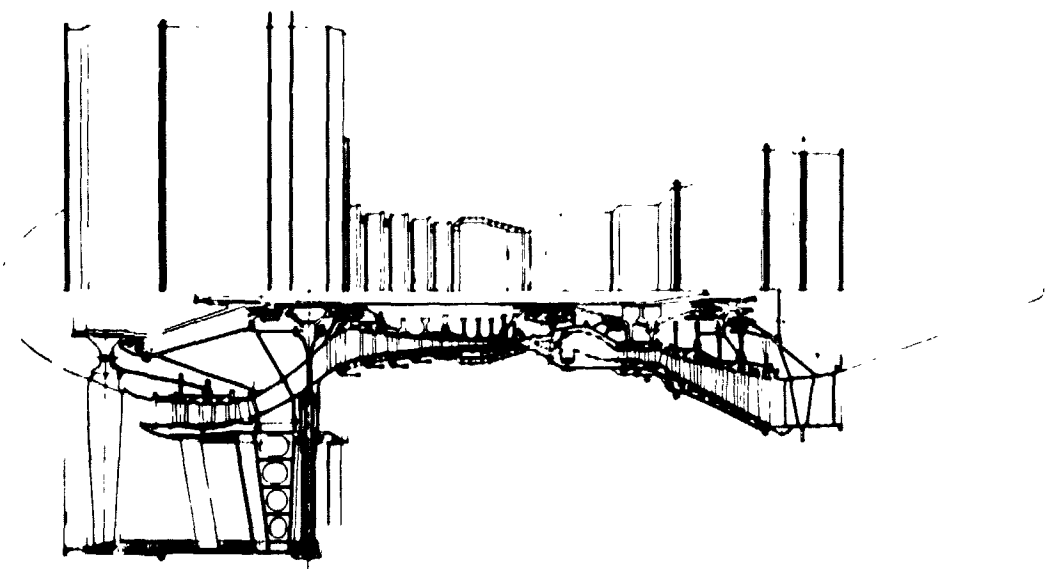

Figure 4 Cross-Section of STF477 Baseline Engine

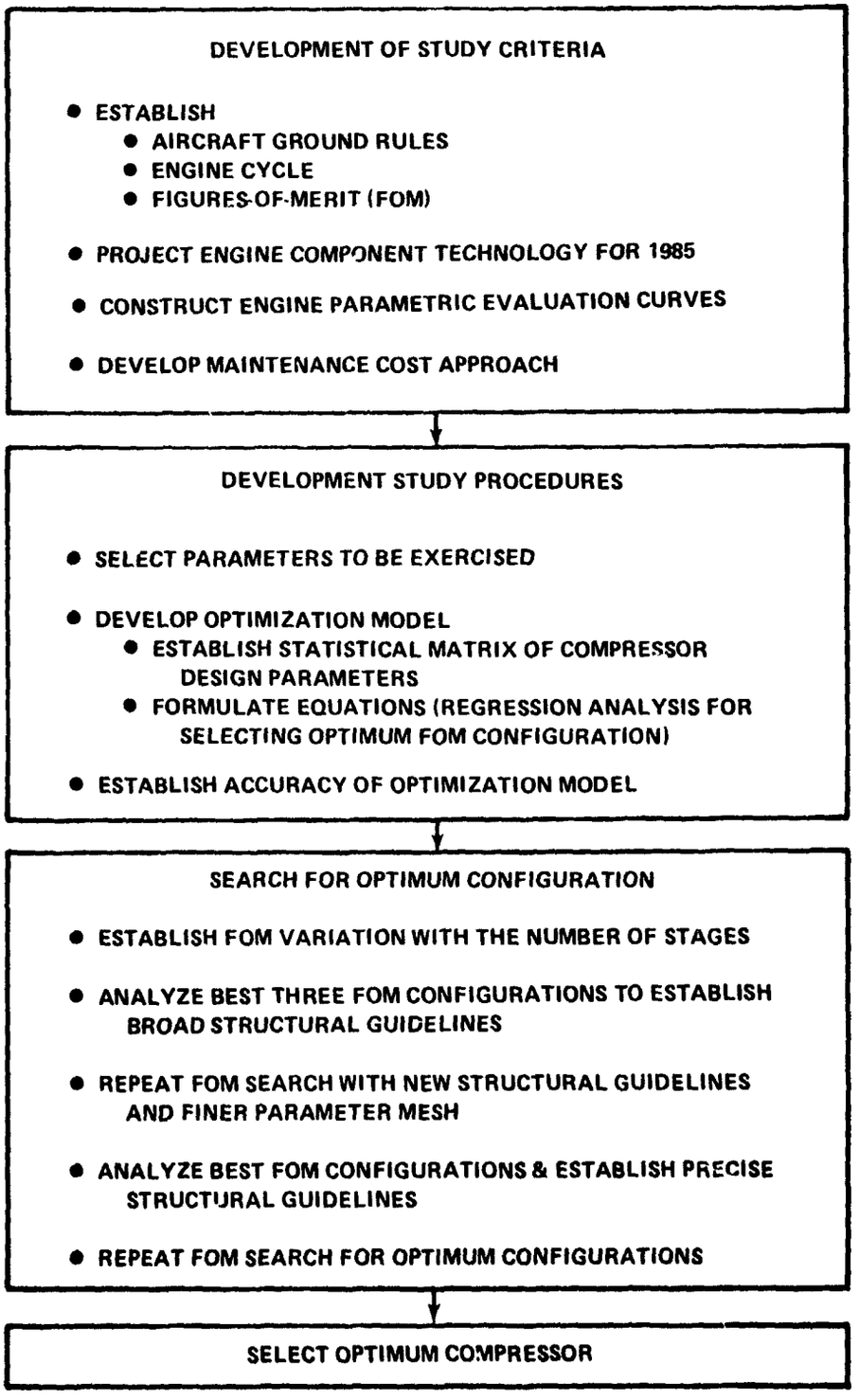

Figure 5 Program Plan Flow Chart

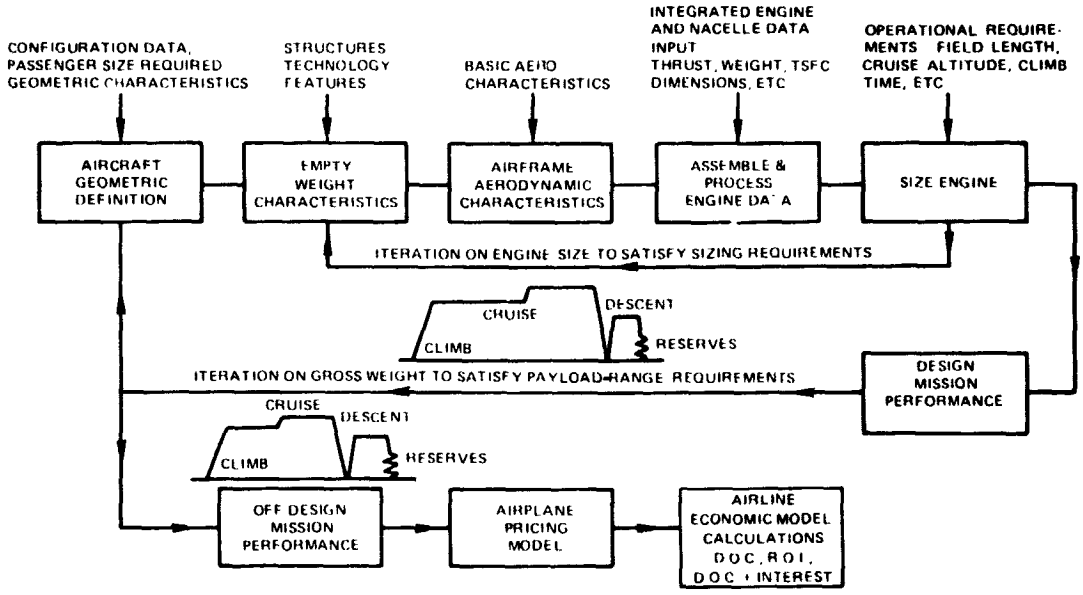

Figure 6 Block Diagram of Vehicle System and Economic Analysis

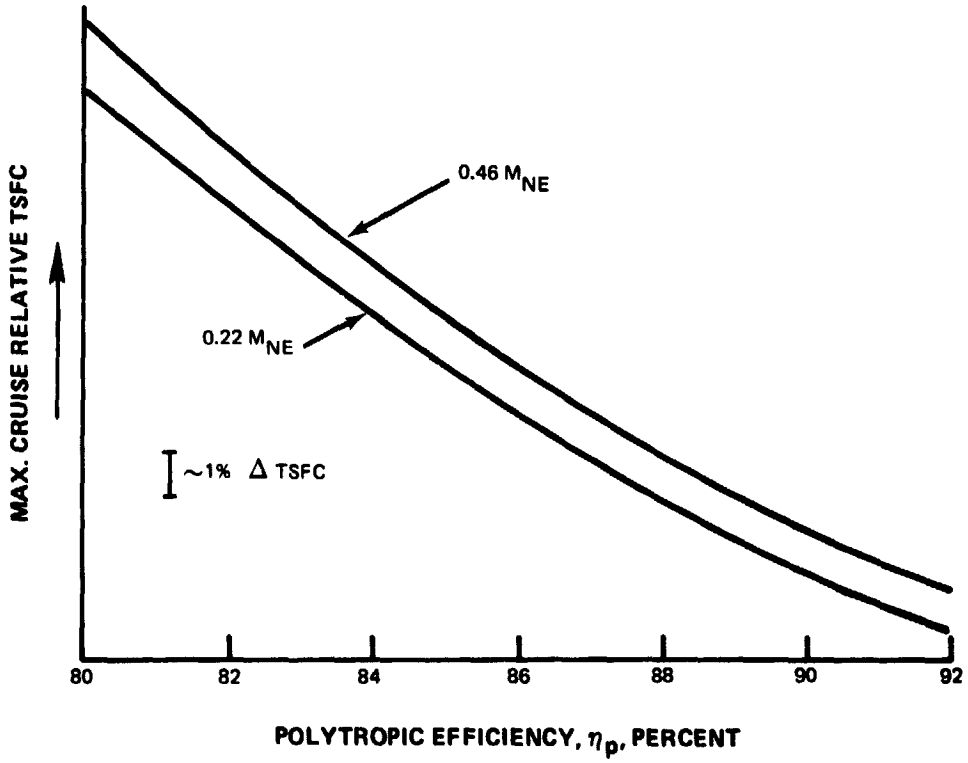

Figure 7 Effects of HP Compressor Polytropic Efficiency and Exit Mach Number on Maximum Cruise Performance at Aerodynamic Design Point

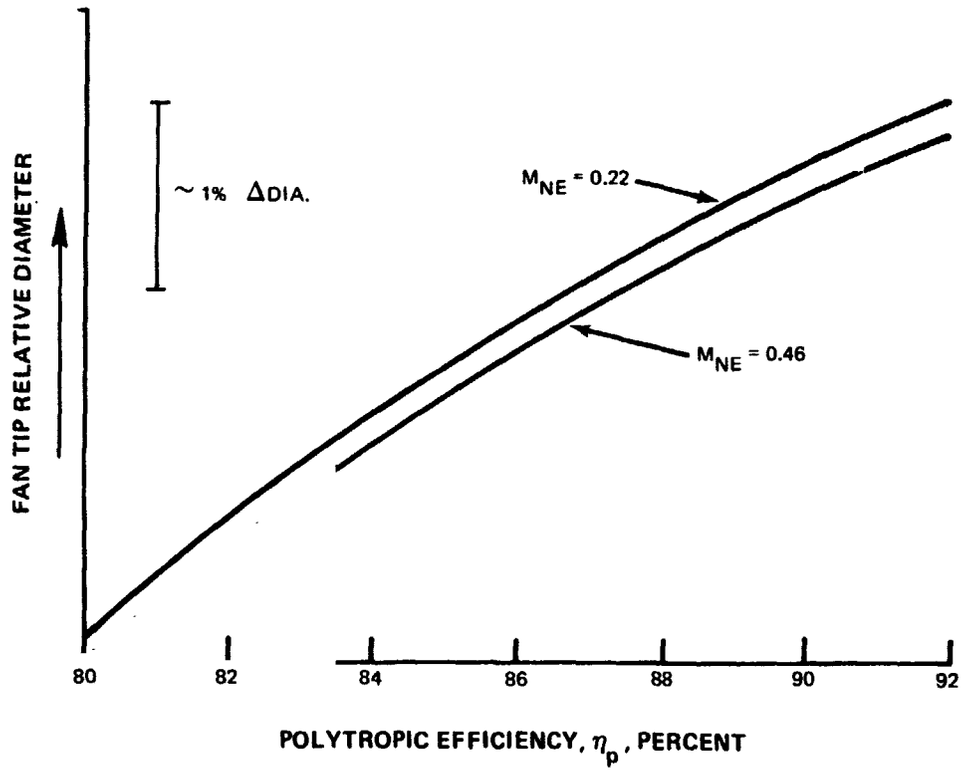

Figure 8 Effects of HP Compressor Polytropic Efficiency and Exit Mach Number on Fan Size

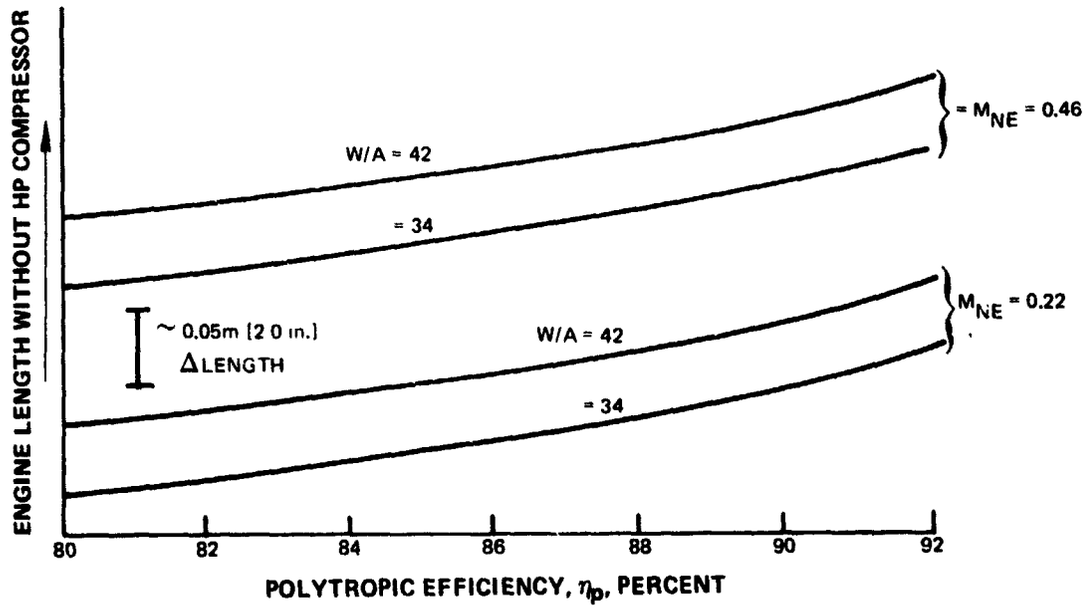

Figure 9 Engine Length (Without HP Compressor) as a Function of HP Polytropic Efficiency for Various Values of Exit Mach Number and Inlet Specific Flow

The aerodynamic flowfield calculation used in this design assumes axisymmetric flow and uses solutions of continuity, energy, and radial equilibrium equations. These equations account for streamline curvature and radial gradients of enthalpy and entropy, but viscous terms are neglected. Calculations were performed on stations oriented at an angle λ with respect to the axial direction.

The equation of motion is in the form of:

$$\frac{1}{2}\frac{\partial V^2_m}{\partial m}\cos(\lambda \quad \epsilon) + \frac{V^2_m}{R_c}\sin(\lambda \quad \epsilon) \cdot \frac{V^2_\theta}{r} + \frac{1}{\rho}\frac{\partial p}{\partial r} = 0$$

$$R_c = \frac{\partial \epsilon}{\partial m} = \text{streamline radius of curvature}$$

Enthalpy rise across a rotor for a streamline ψ is given by the Euler relationship

$$\Delta H_{Rotor} = (U_2 V_{\theta_2})_\psi \quad (U_1 V_{\theta_1})_\psi$$

Weight flow is calculated by the continuity equation

$$W = 2\pi \int_{y\ root}^{y\ tip} \bar{K}\rho V_m \frac{\sin(\lambda - \epsilon)}{\sin\lambda}\, y\, dy$$

where $\bar{K}$ is the local blockage factor and y is the length along the calculation station from the centerline to the point of interest.

Figure 10 Flowfield Calculation Procedure

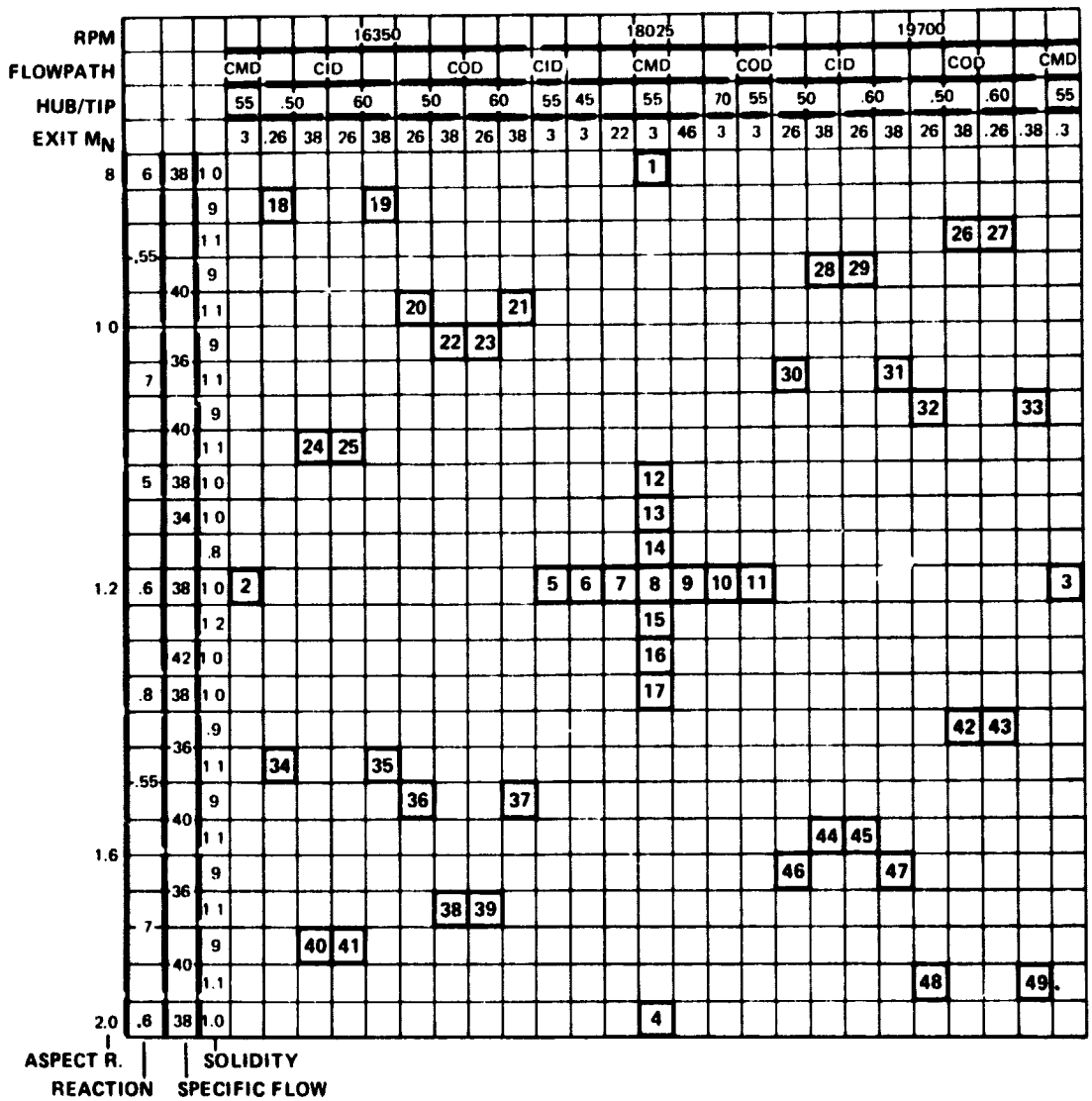

Figure 11 Box-Wilson Statistical Design Matrix

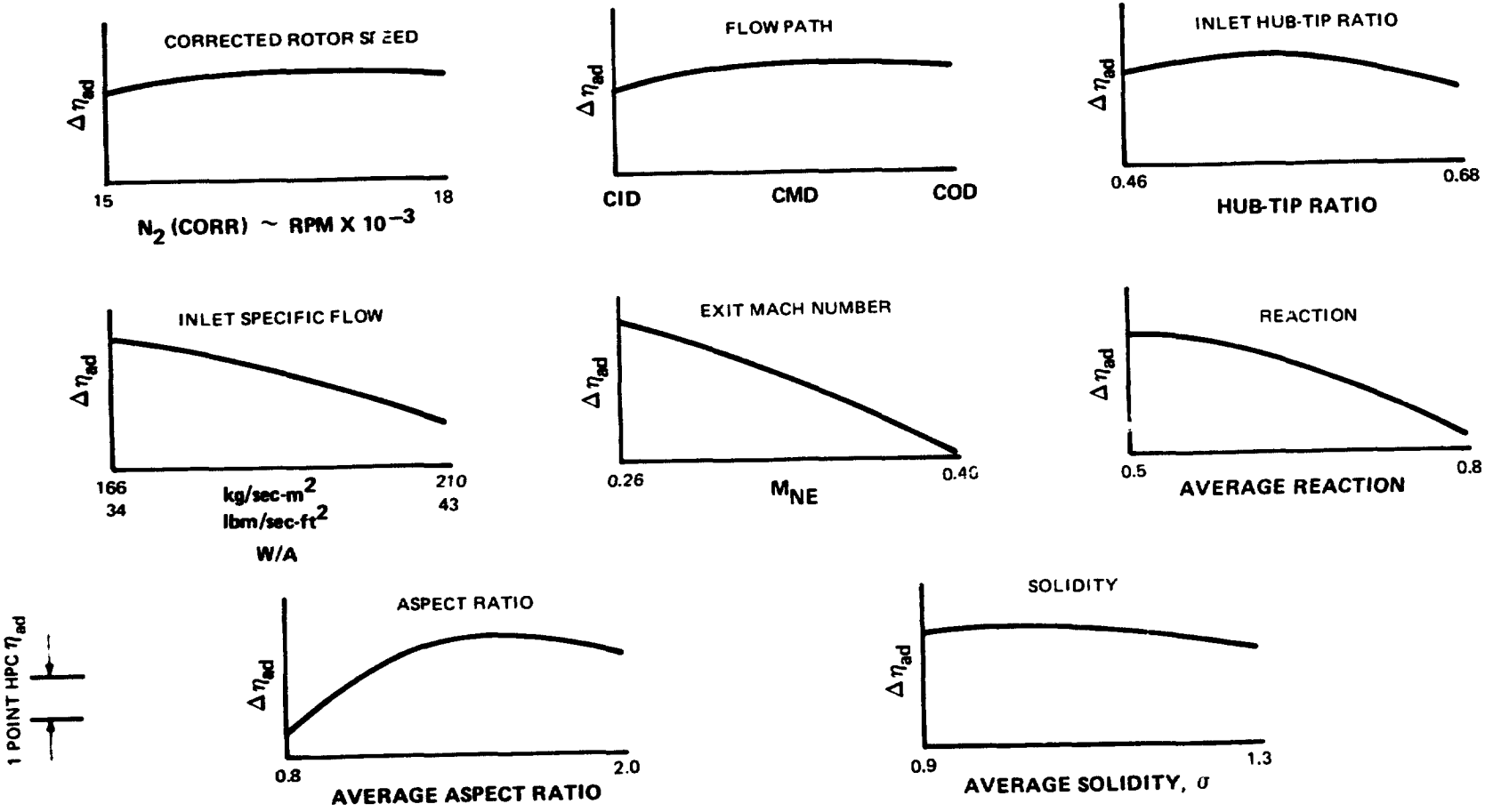

Figure 12 Effects of Various Design Parameters on HP Compressor Adiabatic Efficiency

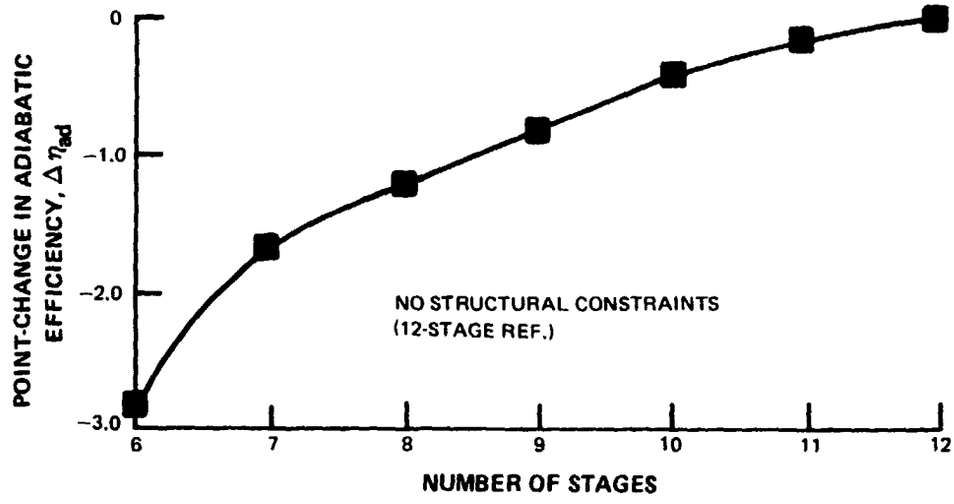

Figure 13 Change in HP Compressor Adiabatic Efficiency Versus Number of Stages; From Regression Analysis

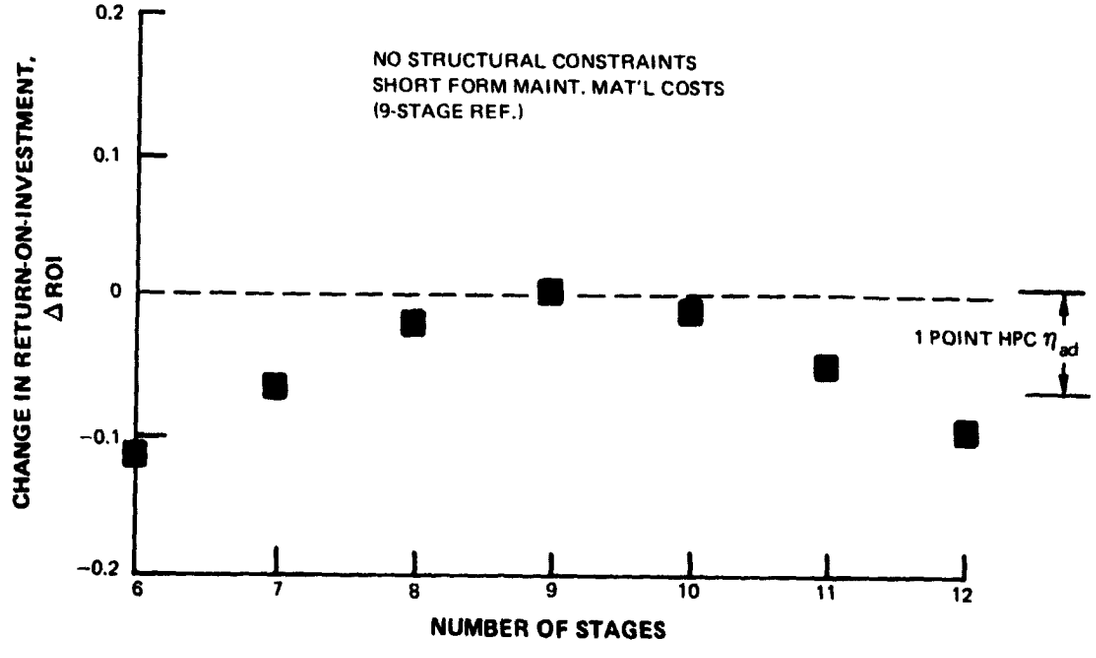

Figure 14 Change in Peak Return-On-Investment Versus Number of Stages; From Regression Analysis

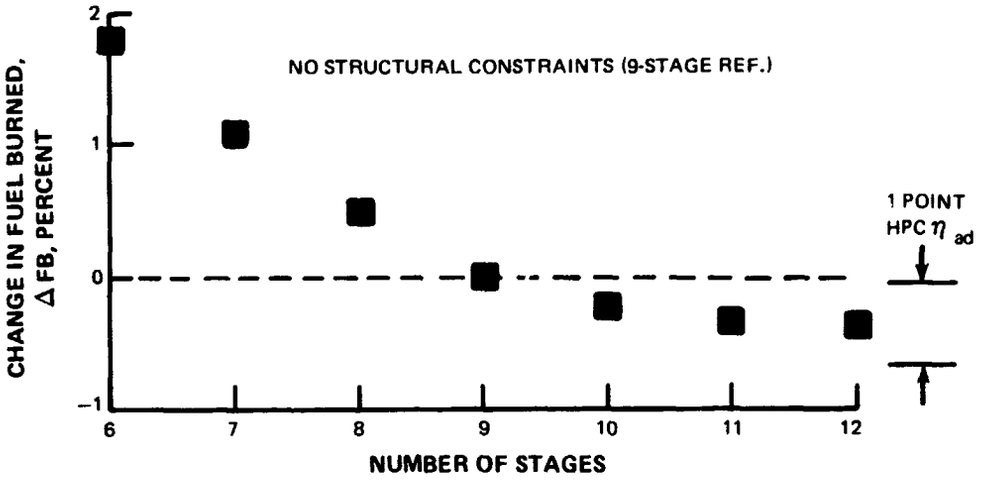

Figure 15 Change in Minimum Fuel-Burned Versus Number of Stages; From Regression Analysis

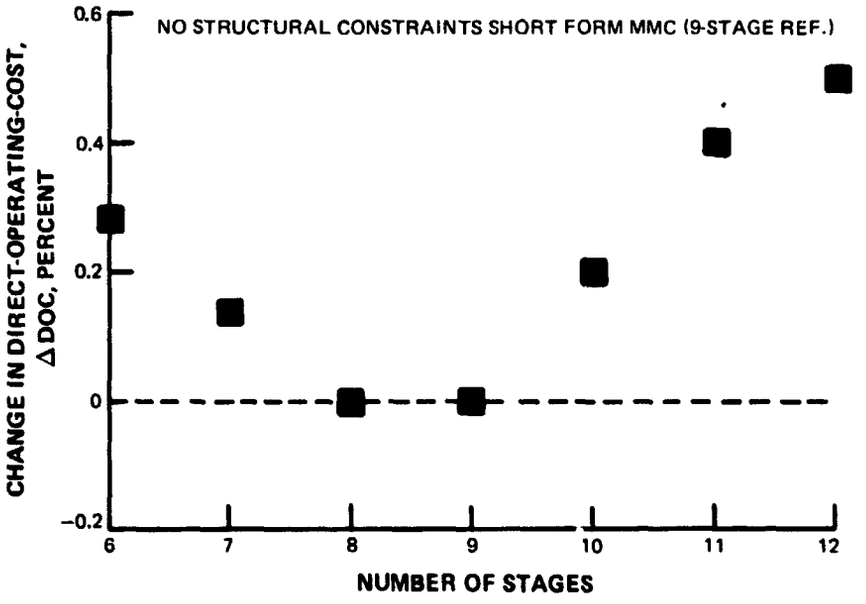

Figure 16 Change in Minimum Direct-Operating-Cost Versus Number of Stages; From Regression Analysis

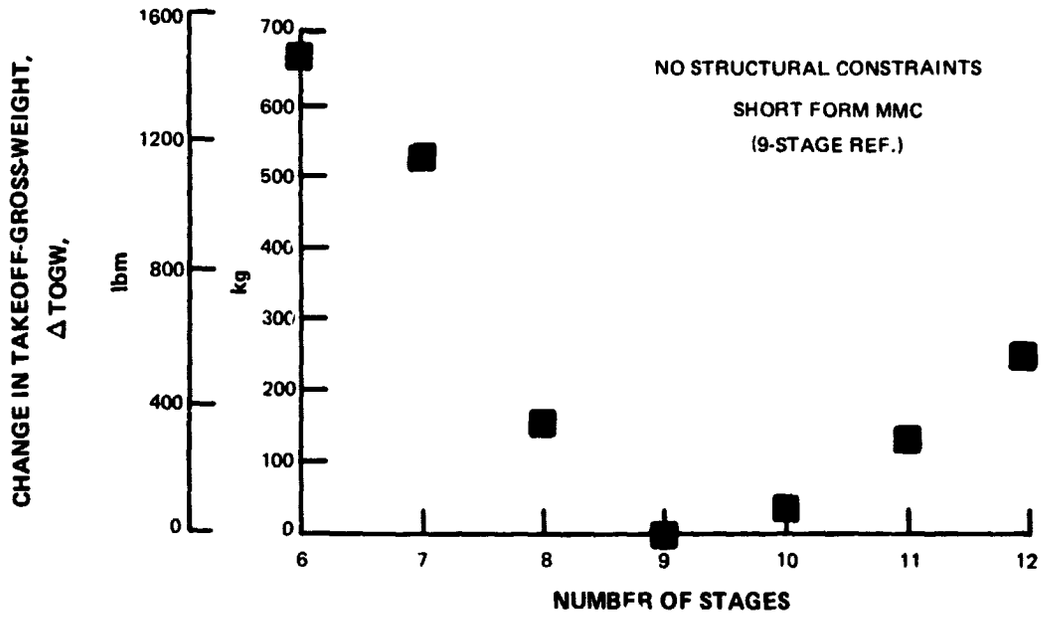

Figure 17 Change in Minimum Takeoff-Gross-Weight Versus Number of Stages; From Regression Analysis

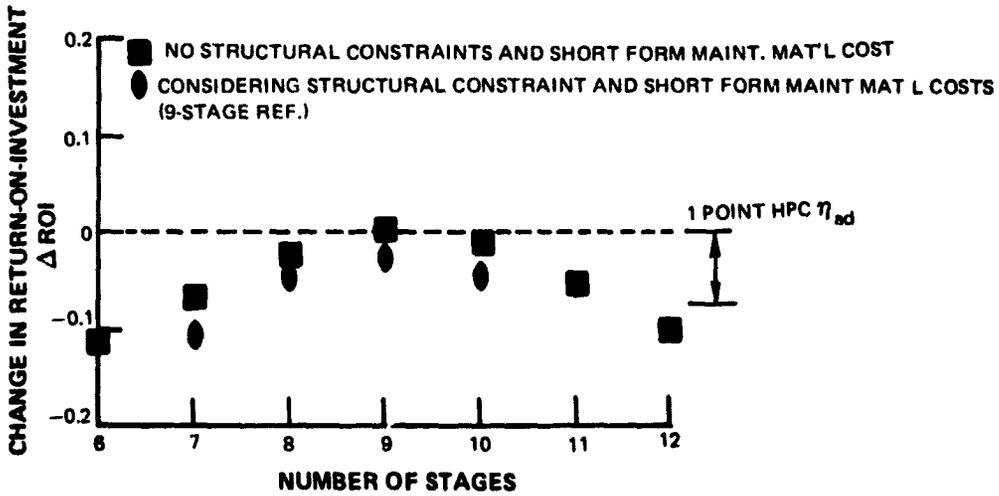

Figure 18 Change in Peak Return-On-Investment Versus Number of Stages; With and Without Structural Constraints

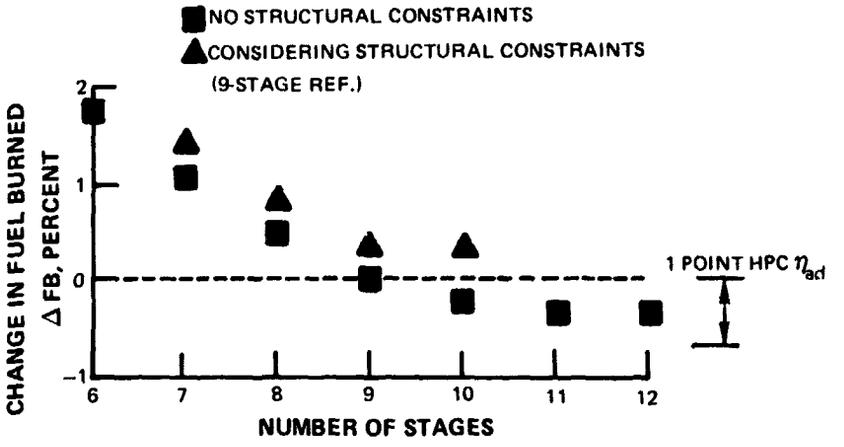

Figure 19 Change in Minimum Fuel Burned Versus Number of Stages; With and Without Structural Constraints

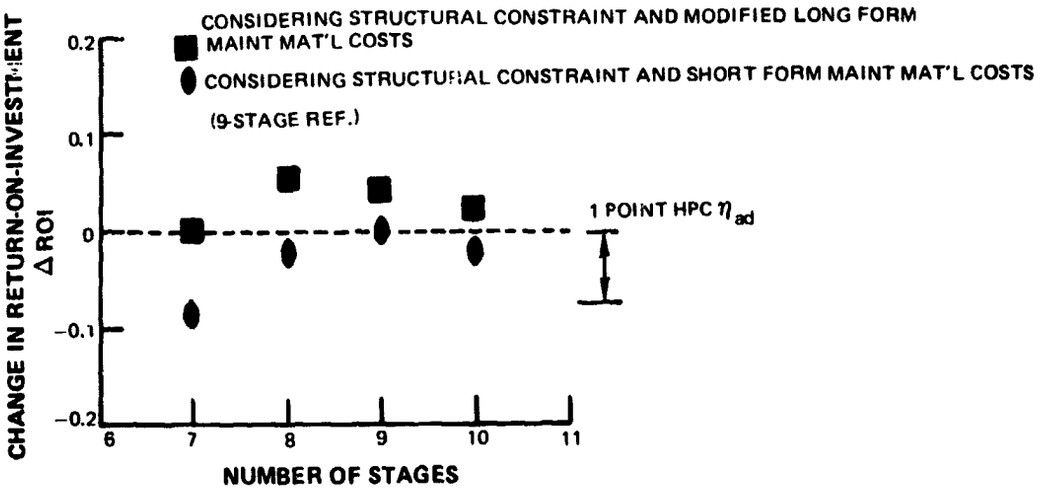

Figure 20 Change in Peak Return-On-Investment Versus Number of Stages; With Short and Modified Long Forms

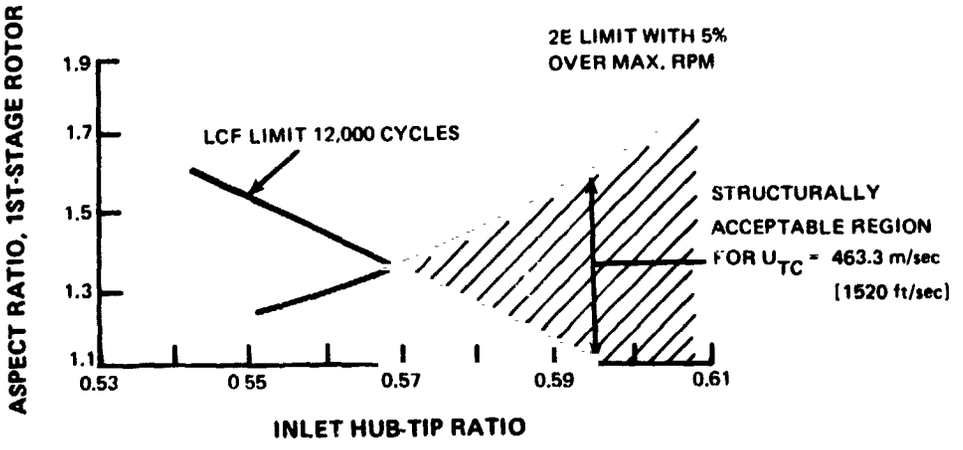

Figure 21 Structurally Acceptable Region for First-Stage Resonance and Allowable LCF Life

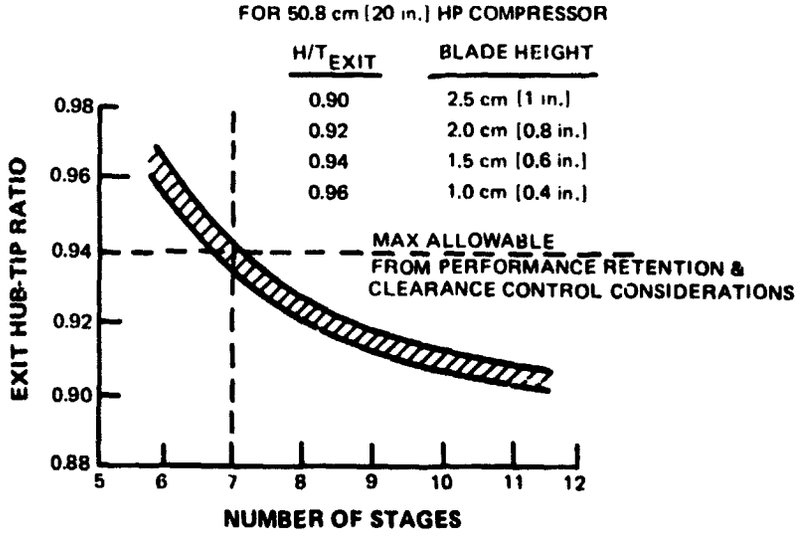

Figure 22 Exit Hub-Tip Ratio Trends Versus Number of Stages

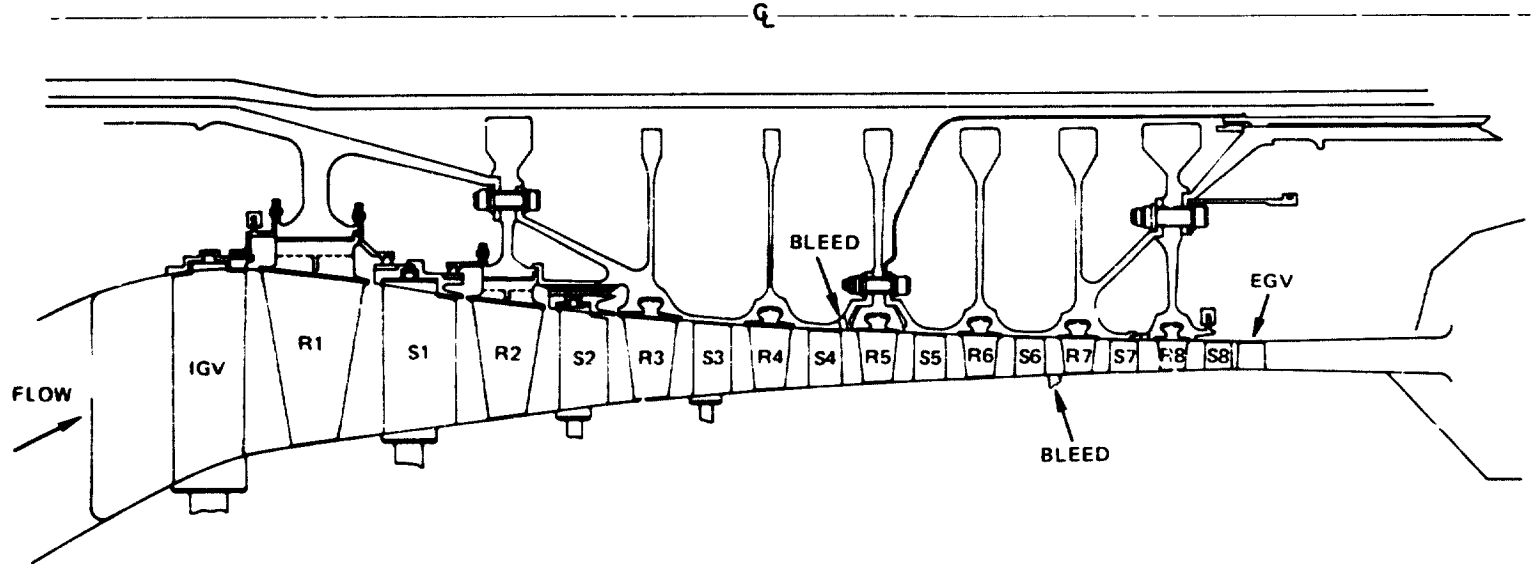

Figure 23 Cross-Section of Selected Eight-Stage Optimum Compressor

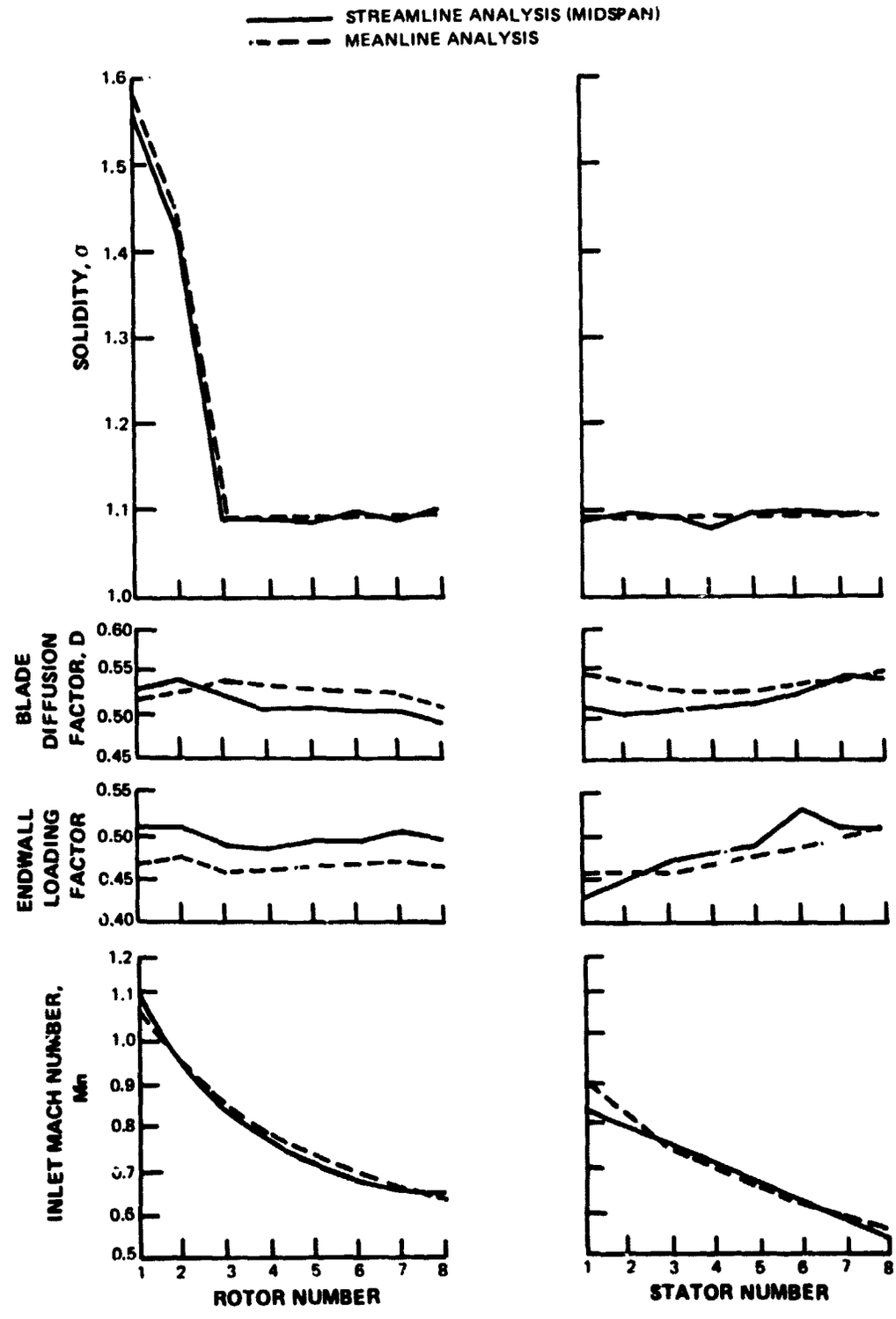

Figure 24 Aerodynamic Parameters From Streamline Analysis for Eight-Stage, Optimum Compressor; Meanline Analysis Results Shown for Comparison

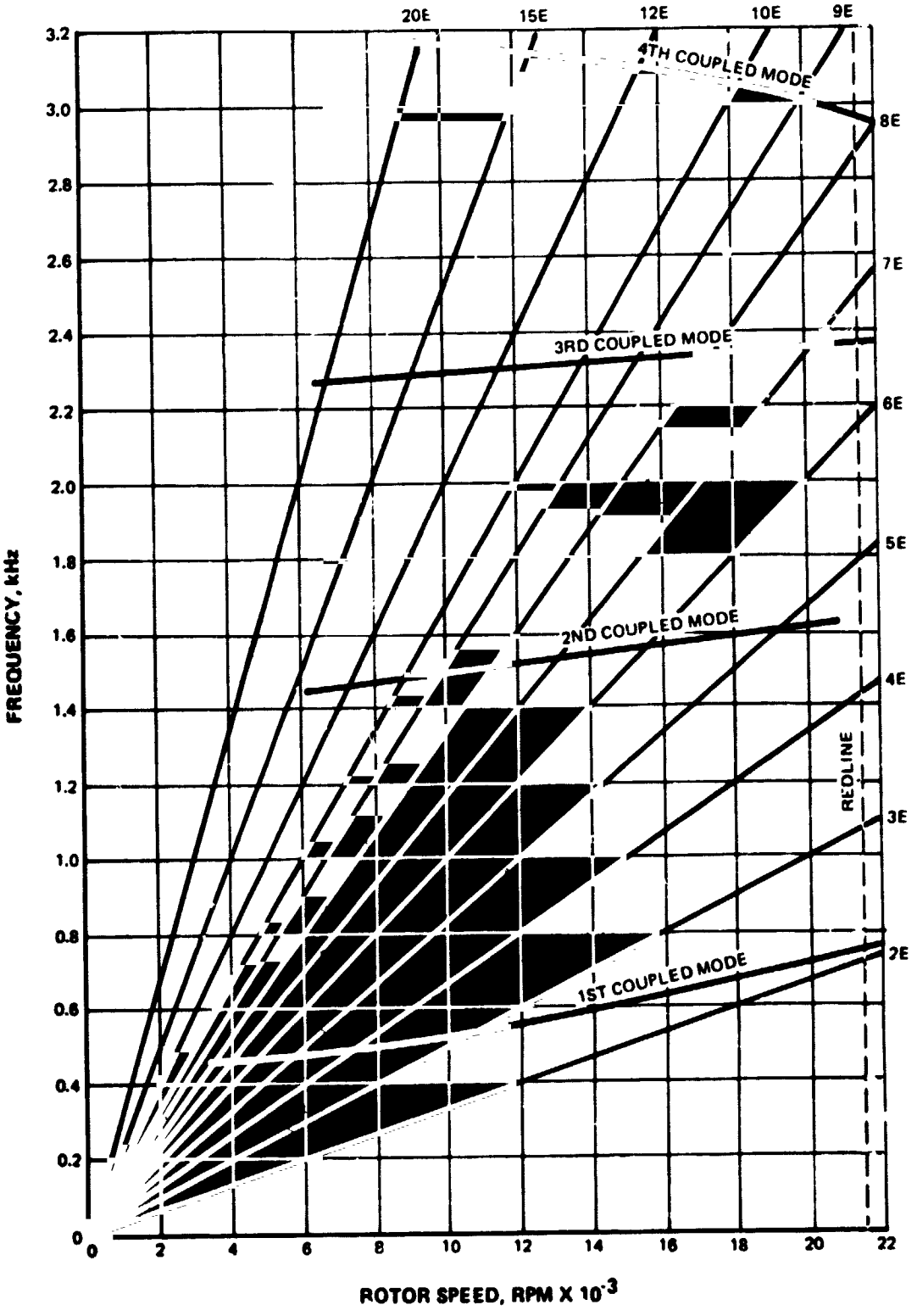

Figure 25 Campbell Diagram for the First-Stage Rotor Blades of the Optimum Compressor

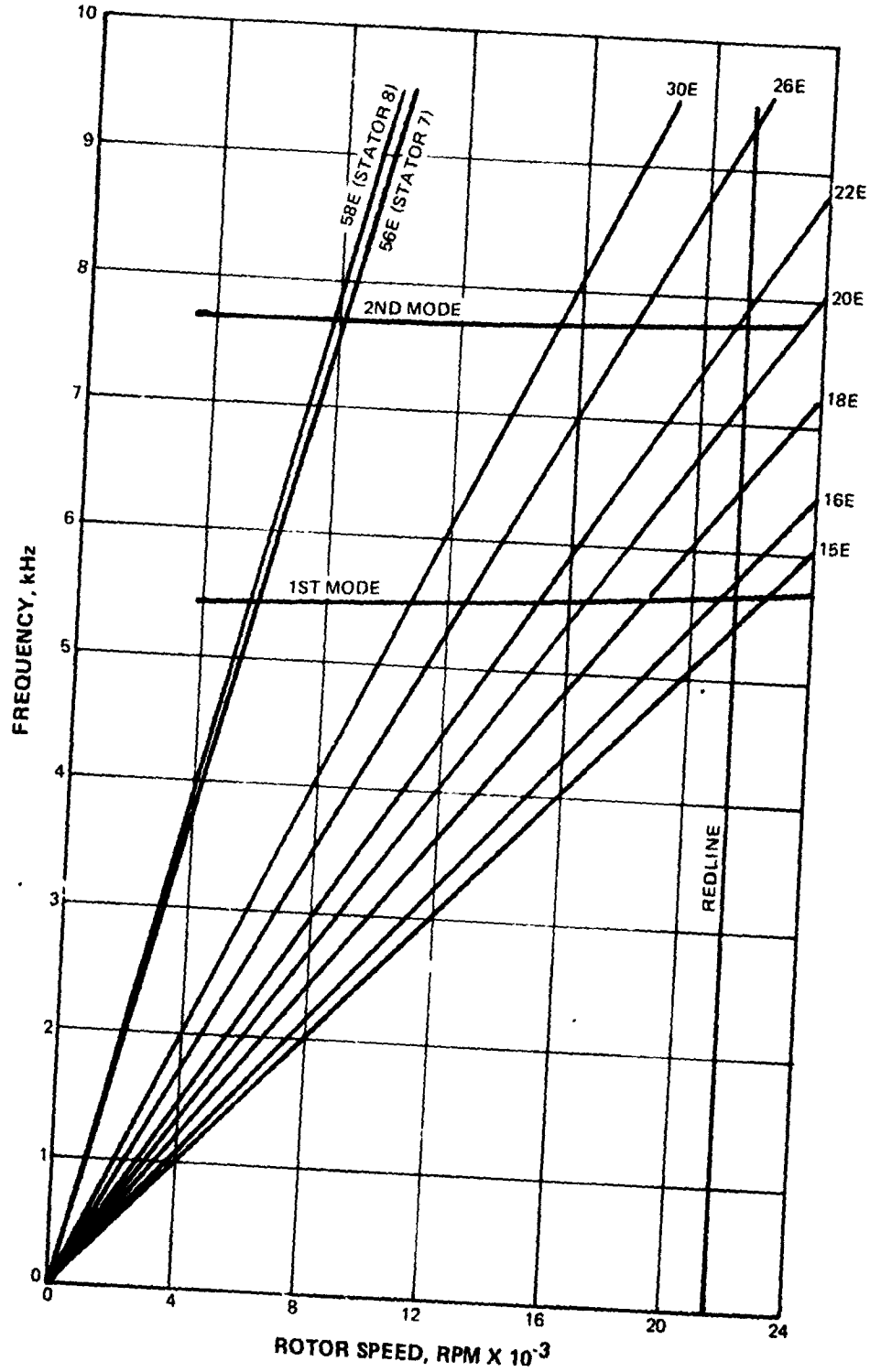

Figure 26 Campbell Diagram for the Eighth-Stage Compressor Blades of the Optimum Compressor

APPENDIX A

ABBREVIATIONS AND SYMBOLS

FB	–	fuel-burned
HP	–	high pressure
ADP	–	aerodynamic design point
CID	–	constant inner diameter
CMD	–	constant mean diameter
COD	–	constant outer diameter
DOC	–	direct-operating cost
EGV	–	exit guide vane
EOH	–	engine operating hours
FOM	–	figure-of-merit
HPC	–	high-pressure compressor
IGV	–	inlet guide vane
LCF	–	low cycle fatigue
MMC	–	maintenance material cost
NOP	–	number of parts
ROI	–	return-on-investment
SEE	–	standard error of estimate
TOGW	–	takeoff-gross-weight
TSFC	–	thrust-specific-fuel-consumption
FAR 36	–	paragraph 36 of Federal Aviation Regulations
D	–	diffusion factor
E	–	excitations per revolution
K	–	number of coefficients
L	–	loading factor
M_{NI}	–	inlet Mach number
M_{NE}	–	exit Mach number
n	–	number of compressor configurations
P	–	total pressure
p	–	static pressure
R	–	reaction
r	–	radius measured from engine centerline
U_{TC}	–	rotor corrected tip speed (tangential)

APPENDIX A (Cont'd)

V_j	–	jet velocity
t/b	–	thickness to chord ratio
T	–	temperature
V′	–	air velocity (rotor)
V	–	air velocity (stator)
W/A	–	inlet corrected specific flow
H/T	–	hub-tip ratio
τ	–	ratio of specific heats for air
η	–	efficiency
σ	–	solidity, ratio of aerodynamic chord to spacing between blades

Subscripts

ad	–	adiabatic (efficiency)
p	–	polytropic (efficiency)
θ	–	tangential component
1	–	inlet
2	–	exit

APPENDIX B

PERFORMANCE PARAMETERS

Polytropic efficiency:

$$\eta_p = \frac{\frac{\gamma - 1}{\gamma} \ln\left(\frac{P_2}{P_1}\right)}{\ln\left(\frac{T_2}{T_1}\right)}$$

Adiabatic efficiency:

$$\eta_{ad} = \frac{\left(\frac{P_2}{P_1}\right)^{(\gamma - 1)/\gamma} - 1}{\left(\frac{T_2}{T_1}\right) - 1}$$

Diffusion factor:

$$D = 1 - \frac{V'_2}{V'_1} + \frac{r_2 V_{\theta 2} - r_1 V_{\theta 1}}{(r_2 + r_1)\sigma V'_1} \quad \text{(rotors)}$$

$$D = 1 - \frac{V_2}{V_1} + \frac{r_1 V_{\theta 1} - r_2 V_{\theta 2}}{(r_1 + r_2)\sigma V_1} \quad \text{(stators)}$$

Endwall loading factor:

$$L = \frac{p_2 - p_1}{P_1 - p_1}$$

Solidity:

$$\sigma = \frac{\text{blade chord}}{\text{circumferential gap between blades}}$$

APPENDIX B (Cont'd)

Thickness-chord ratio:

$$t/b = \frac{\text{blade cross-section max. thickness}}{\text{blade chord}}$$

Stage Reaction:

$$R = \frac{\text{rotor static pressure rise}}{\text{stage static pressure rise}}$$